AKADÉMIAI KIADÓ

Central European Geology

65 (2022) 1, 77–110

DOI: 10.1556/24.2022.00114

RESEARCH ARTICLE

Complex deformation history of the Keszthely Hills, Transdanubian Range, Hungary

GÁBOR HÉJA[1,2*], LÁSZLÓ FODOR[2,3], GÁBOR CSILLAG[3,4], HUGO ORTNER[5] and SZILVIA KÖVÉR[2,3]

[1] Mining and Geological Survey of Hungary, Budapest, Hungary

[2] Eötvös Loránd University, Institute of Geography and Earth Sciences, Department of Geology, Budapest, Hungary

[3] ELKH-ELTE Geological, Geophysical and Space Science Research Group, Budapest, Hungary

[4] Research Centre for Astronomy and Earth Sciences, Institute for Geological and Geochemical Research, Budapest, Hungary

[5] University of Innsbruck, Department of Geology, Innsbruck, Austria

Received: August 6, 2021 • Accepted: February 11, 2022
Published online: April 25, 2022

ABSTRACT

We have investigated the deformation history of the Keszthely Hills (Transdanubian Range, W Hungary), which belongs to the uppermost slice of the Austroalpine nappe system. This Upper Triassic to Upper Miocene sedimentary rock sequence documented the deformation of the upper crust during repeated rifting and inversion events. We investigated the structural pattern and stress field evolution of this multistage deformation history by structural data collection and evaluation from surface outcrops. Regarding the Mesozoic deformations, we present additional arguments for pre-orogenic (Triassic and Jurassic) extension (D1 and D2 phases), which is mainly characterized by NE–SW extensional structures, such as syn-sedimentary faults, slump-folds, and pre-tilt conjugate normal fault pairs. NW–SE-striking map-scale normal faults were also connected to these phases.

The inversion of these pre-orogenic structures took place during the middle part of the Cretaceous; however, minor contractional deformation possibly reoccurred until the Early Miocene (D3 to D5 phases). The related meso- and map-scale structures are gentle to open folds, thrusts and strike-slip faults. We measured various orientations, which were classified into three stress states or fields on the basis of structural criteria, such as tilt-test, and/or superimposed striae on the same fault planes. For this multi-directional shortening we presented three different scenarios. Our preferred suggestion would be the oblique inversion of pre-orogenic faults, which highly influenced the orientation of compressional structures, and resulted in an inhomogeneous stress field with local stress states in the vicinity of inherited older structures.

The measured post-orogenic extensional structures are related to a new extensional event, the opening of the Pannonian Basin during the Miocene. We classified these structures into the following groups: immediate pre-rift phase with NE–SW extension (D6), syn-rift phase with E–W extension (D7a) and N–S transpression (D7b), and post-rift phase with NNW–SSE extension (D8).

KEYWORDS

brittle deformation, Pannonian basin, Transdanubian Range, Keszthely Hills, fault-slip analyses

*Corresponding author. Mining and Geological Survey of Hungary, 17–23 Columbus Str., H-1145 Budapest, Hungary.
E-mail: hejagabor@hotmail.com

INTRODUCTION

The Transdanubian Range (TR) represents the junction of the Eastern Alps and Western Carpathians in the western part of the Pannonian Basin (Fig. 1a), and forms a NE–SW-striking hilly area of Paleozoic and Mesozoic basement rocks surrounded by Eocene to Miocene sediments (Fig. 1b). The structural evolution of the TR and the surrounding Cenozoic basins have been investigated in detail on the basis of field observations (Budai

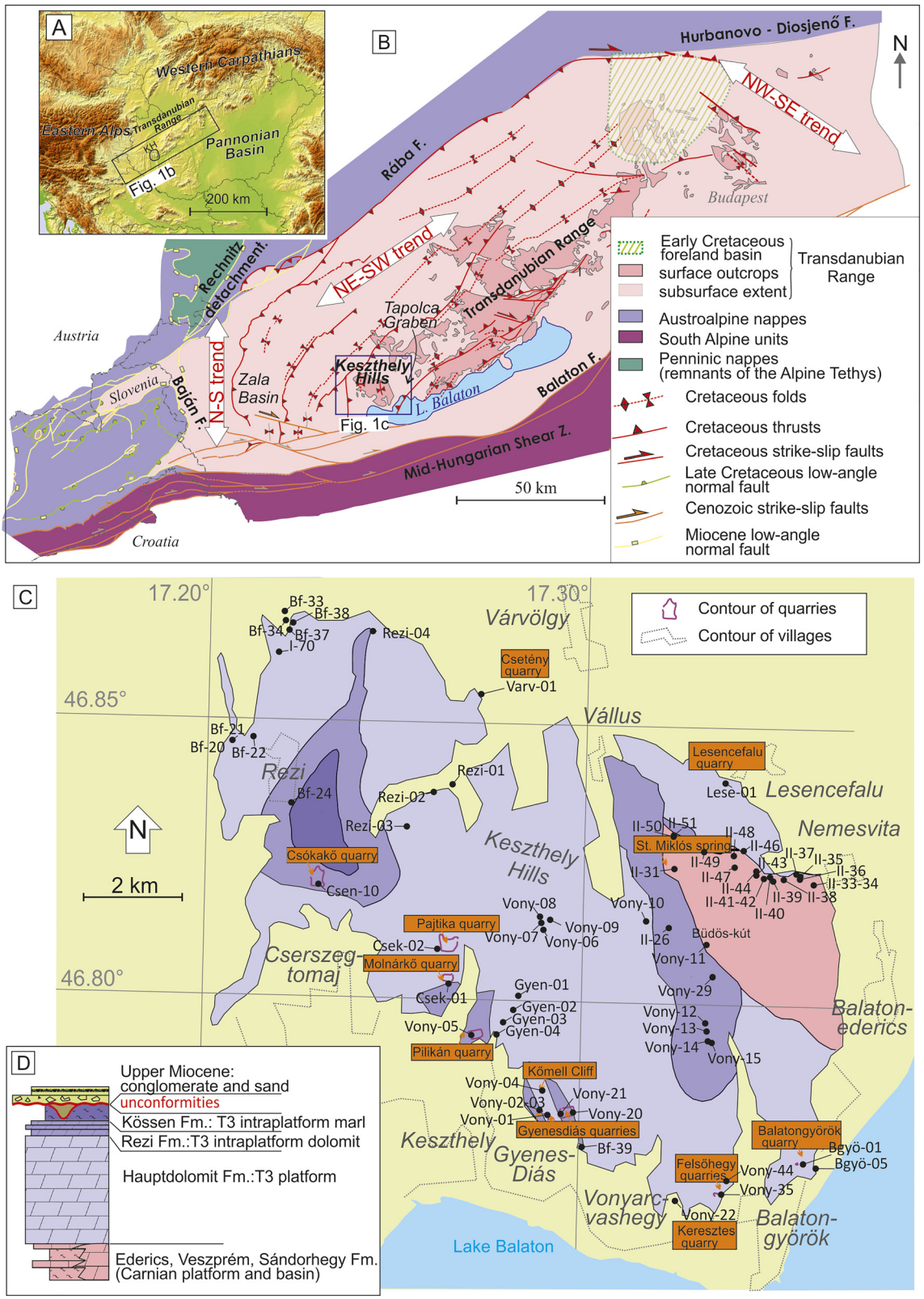

Fig. 1. a) position of the Keszthely Hills (KH) within the Pannonian Basin, b) geometry of major map-view Cretaceous compressional structures of the Transdanubian Range (Fodor et al., 2017, modified), c) location of the investigated big quarries and smaller outcrops on the geologic map of the Keszthely Hills (Budai et al., 1999b, modified), for the legend of the stratigraphic units see Fig. 1d, d) stratigraphy of the KH

et al., 1999a; Sasvári et al., 2007; Fodor, 2008; Kiss, 2009; Fodor et al., 2018), borehole, map and seismic interpretation (Balla and Dudko, 1989; Dudko et al., 1992; Tari, 1994; Tari and Horváth, 2010). However, the Keszthely Hills (KH), which is the westernmost horst of the TR (Dudko et al., 1992), lacks structural data. Only a few publications involved some structural aspects, most of them related to geologic mapping (Szentes, 1957; Bohn, 1979; Dudko et al., 1992; Budai et al., 1999a; Dudko, 1996; Héja, 2015; Héja et al., 2018). This lack of interest was possibly due to the reduced stratigraphy, since the Upper Triassic carbonates are directly overlain by Upper Miocene deposits, which makes the age calibrations for deformation phases difficult (Fig. 1c and d).

In this study, we present a detailed structural documentation of spectacular quarries and other outcrops of the KH. We collected a considerable amount of structural data including faults and associated slickenlines, joints and neptunian dykes, in order to reconstruct the structural evolution based on fault-slip analysis and mapping. Mesozoic structures were the focus of our study, but we analyzed younger deformations, which strongly overprinted the Mesozoic structures.

The TR had a complex structural evolution, with three key events: a) Triassic to Jurassic pre-orogenic extension related to the rifting and opening of the Neotethys and Alpine Tethys oceans, b) mid-Cretaceous main folding phase(s) (broadly between late Aptian and Coniacian), and c) renewed extension, most probably related to the opening of the Pannonian Basin (PB).

All three of them have extensive literature at basin scale, however, open questions have still remained. The repeated pre-orogenic extension prior to Cretaceous folding was postulated based on abrupt facies changes of the Triassic and the Jurassic formations (Galácz and Vörös, 1972; Galácz, 1988; Budai and Vörös, 1992, 1993, 2006; Haas, 1993; Csillag et al., 1995; Vörös and Galácz, 1998; Budai et al., 2001). Generation of joints and fractures combined with fluid flow were connected to this extension, which resulted in vein-formation (Benkó et al., 2014; Molnár et al., 2021). However, pre-orogenic syn-sedimentary faults were rarely observed and measured directly, and the observations mainly depict the Jurassic structures (Lantos, 1997; Fodor 2008; Fodor et al., 2013b). Following the geologic mapping and related studies (Budai et al., 1999a, b) Héja et al. (2018) identified map-scale pre-orogenic normal faults in the study area based on surface observations and interpretation of 2D seismic sections located west of the outcrops. In this paper, we present some additional field data with respect to this early, pre-orogenic extension.

The TR suffered significant shortening during the Cretaceous folding (e.g., Teleki, 1939; Erdélyi Fazekas, 1943; Haas et al., 1984; Tari, 1994; Budai et al., 1999a; Tari and Horváth, 2010; Csicsek and Fodor, 2016; Tari et al., 2021), although the geometry, the style of deformation and the number of folding phases are strongly controversial in different works. Cretaceous contractional structures show various trends (shortening directions) (Fig. 1b), which is traditionally explained by two or even three phases of folding and thrusting in the TR, well separated in time and in tectonic context (Tari, 1994; Csontos and Vörös, 2004; Csontos et al., 2005; Pocsai and Csontos, 2006; Palotai et al., 2006; Sasvári, 2008, 2009; Tari and Horváth, 2010; Fodor et al., 2018; Szives et al., 2018). In contrast, our early results suggested that deviations of fold trends can be explained rather by inheritance of Triassic and Jurassic pre-orogenic normal faults than by multiphase folding (Héja et al., 2016, 2017, 2022). In this work, we document outcrop-scale structures and faults-slip analysis which serve as the basis of this alternative explanation for the number and character of folding phases.

The Miocene extensional Pannonian Basin is a famous example of subduction-related back-arc basins, and it provides an important analogy for other back-arc basins worldwide (e.g., Balázs et al., 2017). Its Miocene tectonic evolution is the topic of a huge number of studies from the 1980s until most recent times (Mészáros, 1982, 1983; Royden, 1988; Rumpler and Horváth, 1988; Tari et al., 1992; Tari, 1994; Csontos, 1995; Fodor et al., 1999; Horváth et al., 2015; Balázs et al., 2016). The TR is densely dissected by syn-rift faults, but structural studies have mainly concentrated on the central and northern parts so far (Bada et al., 1996; Fodor, 2008; Fodor et al., 1994, 2018). East of the KH Dudko et al. (1992) offered a model for basin opening suggesting the connection of transtension, extension and vertical axis block rotation. In the Tapolca Basin the studies of Csillag et al. (2004, 2010) determined the basin-bounding main faults and their timing of activity. Around the study area, Fodor et al. (2021) recently summarized the Badenian to Pannonian structures, basin opening and stress field evolution. This study will present additional field observations and outcrop-scale, detailed fault-slip analysis for this rifting process.

GEOLOGIC SETTING

The study area is the westernmost part of Transdanubian Range Unit (Fig. 1b). Here, the Mesozoic basement is gradually submerging westward below Cenozoic cover (Fodor et al., 2013a). The Transdanubian Range (TR) is built up by low-grade metasediments and metavolcanites, metamorphosed during the Variscan orogeny, and a Permian to Cenozoic non-metamorphosed succession.

The oldest known formations in the KH are the heteropic Carnian Veszprém Marl Fm and Ederics Limestone Fm, which were deposited respectively in an intraplatform basin and a carbonate platform environment (Góczán et al., 1983; Csillag et al., 1995; Haas et al., 2014) (Fig. 1d). The Ederics Limestone Fm is made up of thick-layered limestone that suffered partial dolomitization (Haas et al., 2014). This platform laterally interfingers with the basinal marly succession of the Veszprém Marl and Sándorhegy formations. Limited occurrences of proximal slope breccias were documented in the KH (Csillag et al., 1995).

From the end of the Carnian the depositional environment became uniform and the Hauptdolomit Fm was

Table 1. WGS84 coordinates of the investigated outcrops

Name of the outcrop	Latitude (northing) in degree	Longitude (easting) in degree	Name of the outcrop	Latitude (northing) in degree	Longitude (easting) in degree
II-26	46.81279	17.3223	Csen-10 (Csókakő quarry)	46.82219	17.2310
II-31 (St Miklós spring)	46.82416	17.3226	Gyen-01	46.80057	17.2823
II-33	46.82325	17.3628	Gyen-02	46.79800	17.2810
II-34	46.82322	17.36110	Gyen-03	46.79573	17.2782
II-35	46.82158	17.3588	Gyen-04	46.79403	17.2768
II-36	46.82129	17.3582			
II-37	46.82153	17.3559	Vony-02 (Gyenesdiás western quarry)	46.77971	17.2896
II-38	46.82111	17.3538	Lese-01	46.83977	17.3354
II-39	46.82080	17.3510	Csek-01 (Molnárkő quarry)	46.80354	17.2647
II-40	46.82165	17.3503	Csek-02 (Pajtika quarry)	46.80990	17.2645
II-41	46.82186	17.3498	Rezi-01	46.83836	17.2636
II-42	46.82211	17.3487	Rezi-02	46.83715	17.2589
II-43	46.82200	17.3467	Rezi-03	46.83463	17.2530
II-44	46.82241	17.3469	Rezi-04	46.86637	17.2413
II-46	46.82625	17.3425	Varv-01	46.85507	17.2722
II-47	46.82332	17.3400	Vony-01 (Gyenesdiás middle quarry)	46.77895	17.2913
II-48	46.82541	17.3399	Vony-03 (Kőmell Cliff)	46.77971	17.2896
II-49	46.82628	17.3321	Vony-05 (Pilikán quarry)	46.79338	17.2725
II-50	46.82917	17.3243	Vony-07	46.81439	17.2890
II-51	46.82920	17.3238	Vony-09	46.81490	17.2913
II-70	46.83066	17.3211	Vony-10	46.81411	17.3164
Bf-20	46.84225	17.1933	Vony-11	46.80950	17.3320
Bf-21	46.84564	17.2053	Vony-12	46.79546	17.3311
Bf-22	46.84539	17.2084	Vony-13	46.79398	17.3314
Bf-23	46.84643	17.2110	Vony-14	46.79221	17.3316
Bf-24	46.83454	17.2211	Vony-15	46.79197	17.3324
Bf-33	46.86912	17.2182	Vony-02	46.77991	17.2901
Bf-34	46.86855	17.2187	Vony-20 (Gyenesdiás eastern quarry)	46.77917	17.2970
Bf-35	46.86756	17.2187	Vony-21 (Gyenesdiás eastern quarry)	46.77778	17.2912
Bf-36	46.86582	17.2197	Vony-21	46.77640	17.2870
Bf-37	46.86430	17.2211	Vony-22	46.76398	17.3218
Bf-38	46.86549	17.2215	Vony-29	46.80465	17.3334
Bf-39	46.77619	17.2963	Vony-32	46.79104	17.3370
Bgyö-01 (Balatongyörök quarry)	46.77106	17.3581	Vony-35 (Felsőhegy quarry)	46.76527	17.3367
Bgyö-05 (Szépkilátó)	46.77053	17.3614	Vony-44	46.76765	17.3373

deposited on a huge carbonate platform (Fig. 1d). The formation is built up by thin-layered light grey dolomite in the study area. Occasionally, microbialite intercalations occur. The formation was deposited in a back-reef lagoon environment (Fruth and Scherreiks, 1984), indicating the recovery of arid climate (Haas et al., 2012).

From the end of the Middle Norian (Budai and Kovács, 1986) intraplatform basins opened, and some of them persisted into the Rhaetian. These intraplatform basins were filled up by the late Middle to Upper Norian Rezi Dolomite and the latest Norian–Rhaetian Kössen Marl (Budai and Kovács, 1986; Budai and Koloszár, 1987; Budai et al., 1999a; Haas, 1993; Csillag et al., 1995; Haas et al., 2021). The Rezi Formation is composed of dark-grey cherty, bituminous laminated dolomite with porous dolomite intercalations. A dolomite breccia lithofacies was identified by Csillag et al. (1995) in the Csókakő quarry (KH). This dolomite breccia is made up of dolomite blocks redeposited from the coeval platform into a shallow basin marked by laminated dolomite matrix.

The rest of the Mesozoic succession was eroded by multiple denudation phases during the mid-Cretaceous – Miocene interval, which resulted in a uniform, flat-lying erosional surface. The continental Cserszegtomaj Kaolinite was deposited in deep karstic sinkholes of this denudation surface in the KH (Szentes, 1957; Bárdossy, 1959; Csillag, 1959; Bohn, 1979; Csillag and Nádor, 1997; Budai et al., 1999a) which is Badenian in age (Kelemen et al., 2021); kaolinite deposition was partly coeval with marine sediments of the grabens around the KH (Fodor et al., 2021).

The transgression of Lake Pannon reached the area of the KH only during the Late Miocene (Fig. 1d). Most of the area was covered by clastic deltaic sediments (Újfalu Fm) of Lake Pannon. On the steep slopes of the graben boundaries abrasion-related, coarse-grained gravels were formed (Békés Fm, Diás Mb.), which were usually cemented onto the Triassic dolomite surface. Narrow and relatively deep valleys within the hilly regions were the location of travertine production (Nagyvázsony Fm) during the final stage of deltaic sedimentation (Budai et al., 1999a).

METHODOLOGY

We made detailed structural observations in the quarries and natural outcrops of the Keszthely Hills (KH). For locations of the outcrops see Fig. 1c and Table 1. Several types of structural data (bedding, faults, joints, neptunian dykes, veins, deformation bands) were measured in the outcrops of the KH, which were plotted using the software of Angelier (1990) (for legend see Fig. 2c). All the data were illustrated by stereoplots, with lower hemisphere equal area projection.

Estimation of the principal stress axes was prepared using the theory of conjugate fractures of Anderson (1951). In rare cases, when only one phase affected the rocks, direct stress tensor calculation was executed by the "Tensor"

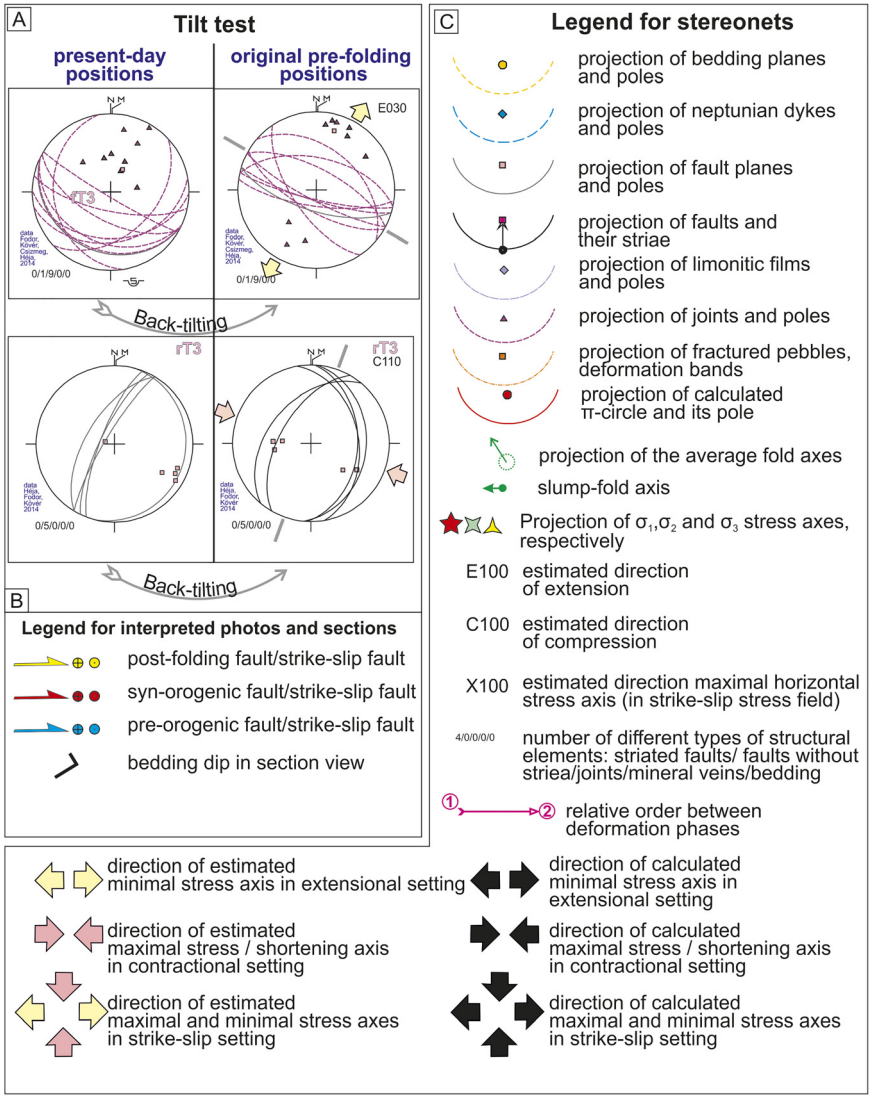

Fig. 2. a) Two examples of the applied tilt-tests. In the first row, flatly to steeply southerly dipping set of joints form nice extensional Mohr-pairs before folding. Steep and flat faults form nice conjugate thrust planes prior to tilting, as shown in second row; b) legend for outcrop structures c) legend for stereoplots

module of Angelier (1984, 1990). Fault-slip inversion and automatic separation of phases was carried out using the "Phases" module (Angelier and Manoussis, 1980), and this was supplemented by "manual" separation, searching for conjugate fracture sets (Fodor, 2010). The RUP and ANG values are markers for the characterization of stress tensor estimations. The RUP value characterizes the relationship between the measured fault-slip data and the computed shear stress vector (RUP value over 50 and 75 percent indicate moderate and important misfit, respectively) (Angelier, 1990). The ANG value is the angular difference between the measured striae and the computed "ideal" slip vector (ANG value above 22.5° and 45° indicate moderate and important misfit, respectively) (Angelier, 1990). The number of fault-slip data, that show misfit in RUP and ANG values are indicated by exclamation marks (e.g., 3! = 3 faults show moderate misfit; 2!! = 2 faults show important misfit). The phi (Φ) value characterizes the anisotropy of the calculated stress field, where $\Phi = \sigma_2-\sigma_3/\sigma_1-\sigma_3$.

The relative order of the deformation phases was determined by a) cross-cutting relationships, such as overprinting slickenlines (e.g., normal slip overprinted by strike-slip), b) oblique striae on conjugate fault pairs or c) tilt-test. In case b), the oblique slickenlines can be interpreted as a second phase reactivating an older conjugate fault pair with pure dip-slip or strike-slip motion. Case c) tilt test was always made on all fractures using the "Rotilt" module of Angelier (1990).

During this test, all the structural elements were back-tilted to the original, horizontal position of the bedding. Structural elements measured on fold limbs were back-tilted separately, for each limb. The symmetry plane of a conjugate fracture set is considered vertical or horizontal, and the characteristic dip angle of normal, thrust or strike-slip faults are around 60, 30, 90°, respectively. Considerable deviation from these geometries may indicate fault reactivation and/or tilting after fracturing (Fig. 2a). The other basic assumption of the tilt test is that the tilting of the Triassic strata is mostly the result of Cretaceous folding. Consequently, the tilt test gave a relative chronology with respect to tilting/folding. In the case of positive tilt-test, we interpreted the fault pair as pre-tilt or pre-folding structure.

We highlighted with orange color those faults, which play an important role in the determination of the relative order of phases. For example, dip-slip faults (highlighted by orange color) on Fig. 10r show the back-tilted position of oblique-slip faults of Fig. 10x. Another example is Fig. 10a and b, where we assumed that the fault planes (without preserved slickensides) of oblique slip faults (Fig. 10a) formed during an older phase (Fig. 10b).

Several second-order outcrop-scale folds were measured in the dolomite quarries of the KH. Since cylindrical fold geometry was supposed, a best-fitting great circle (π-circle) for the bedding poles were calculated using the InnStereo software developed by Tobias Schönberg in 2015. The pole of this great circle represents the axis of the fold.

Map varieties of this study (Figs 19–22 and 24) were based primarily on the 1:50.000 scale geologic map of the region, published by Budai et al. (1999b). We also used the observation maps which served as basis for the printed map (Bence et al., 1982; Miszlivecz et al., 1982; Budai and Muntyán, 1983; Csillag et al., 1983). The map version of the TJAM project was also used (Fodor et al., 2013a). The fault pattern and geomorphological observations of Csillag and Nádor (1997) were important for the map of the Late Miocene deformation. These data were summarized by Fodor et al. (2021) and modified in this work.

STRUCTURAL OBSERVATIONS IN THE KESZTHELY HILLS (KH)

Csókakő quarry (Csen-10)

Most of the quarry is made up by Rezi Dolomite. Sedimentary breccia interfingering with laminated dolomite was described by Csillag et al. (1995) and Héja et al. (2018) on the eastern wall of the quarry. This special type of Rezi Dolomite is interpreted by these authors as fault-bounded talus breccia in the hanging wall of a major Late Triassic normal fault. A detailed description of the eastern wall of the quarry can be found in the paper of Héja et al. (2018). A recent study indicates that dolomitization of the matrix and the blocks themselves can be related to fault-driven fluid flow (Haas et al., 2021).

There is an almost N–S-striking neptunian dyke on the top of the western wall (Fig. 3a and d). The fissure runs across the Rezi Dolomite, and it is filled up with yellowish-brown quartz sand that we considered to be Late Miocene (Pannonian) in age (Fig. 3a). The neptunian dyke is capped by a strongly cemented iron crust (Fig. 3a). Only one normal fault was measured on the Rezi Dolomite in the quarry, which runs parallel to the neptunian dyke (Fig. 3d).

Pajtika quarry (Csek-02)

This huge quarry is made up of Hauptdolomit (Fig. 4a and b). The strata dip moderately to steeply toward NW to SW in general (Fig. 4d). On the east-facing wall of the quarry a 300 m-wide segment of the gentle, rounded Pajtika syncline is outlined (Fig. 4b). Dip data suggest that the axis of this syncline is plunging significantly toward WSW (Fig. 4d).

A steep NE–SW-striking fault (Fpaj3 on Fig. 4a and e) can be traced on the southern wall of the quarry. The fault core is represented by a 1.5-meter-wide powdered dolomite zone (Fig. 4a). The hanging wall of the Fpaj3 fault is built up by strongly fractured dolomite, representing the few-meter-wide damage zone. In contrast to the hanging wall, the footwall was deformed less intensively. The west-dipping beds show different dips on the two sides of Fpaj3 fault (Fig. 4a). In the northwestern part, the beds dip moderately to the W, whereas at the other side the beds are sub-vertical (Fig. 4a). These sub-vertical beds represent the steep northwestern limb of the rounded Apaj1 anticline. There is no information about the southeastern limb of this anticline, since the quarry terminates at the crest of the fold (Fig. 4a).

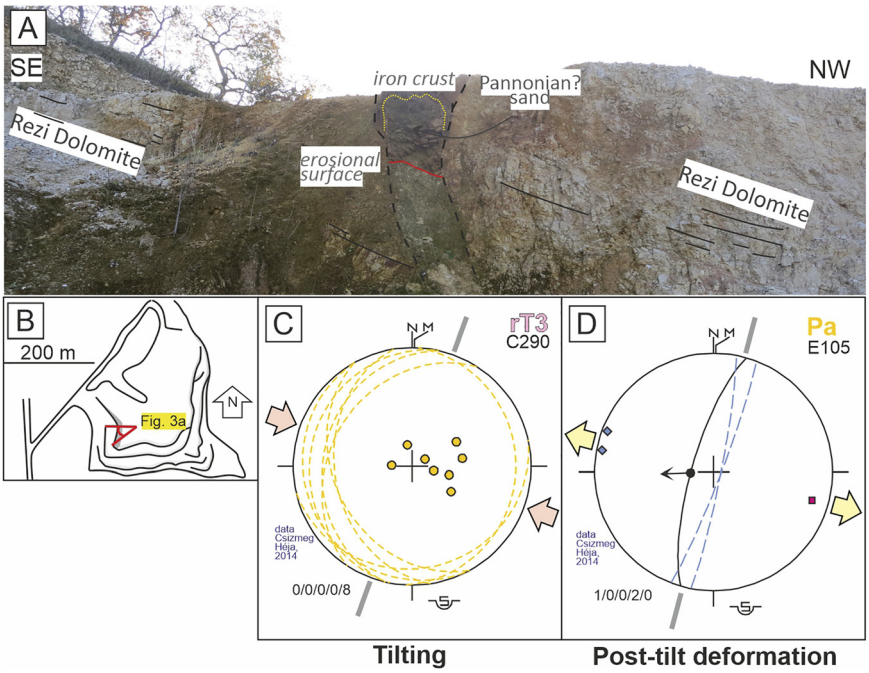

Fig. 3. a) Late Miocene neptunian dyke on the western wall of the quarry b) the position of Fig. 3a in the quarry c) stereoplot of bedding dips measured on the Rezi Dolomite d) stereoplot of the neptunian dyke and a post-tilt normal fault. For location of the outcrop, complete data set, legend for the stereoplots see Fig. 1c, Suppl. I. and Fig. 2c, respectively

The Apaj1 anticline is dissected by several minor thrusts that we were not able to measure (Fpaj4 set on Fig. 4a).

Tilted beds of the Hauptdolomit are dissected by several conjugate thrusts, which developed most possibly after the tilting/folding (e.g., the E-dipping Fpaj2 on Fig. 4a). Occasionally, layer-parallel slickenlines also occur. A part of these structures came into being due to WNW–ESE shortening. NNW–SSE-striking sinistral and WSW–ENE-striking dextral strike-slip faults suitably fit into the related stress field (Fig. 4e). Another set of conjugate thrust faults suggests NE–SW shortening (Fig. 4f). We observed several post-tilt normal faults (e.g., Fpa1j on Fig. 4a), which, together with a few NW–SE striking dextral strike-slip faults, suggest E–W extension with transtensional character (Fig. 4g).

Molnárkő quarry (Csek-01)

Most of the quarry is made up by Hauptdolomit, while in the southeastern corner thinly-bedded, laminated Rezi Dolomite occurs (Fig. 5a). In the Rezi Dolomite few decimeter-wide folds occur. One of these folds is an isoclinal synform, which is outlined only in the laminated dolomite intercalation (Sm1 on Fig. 5b). Despite isoclinal folding, the laminae are not fractured, and show continuous deformation. This laminated dolomite intercalation pinches out toward the SE, between two layers of dolomite. The axial plane of the Sm1 synform is dipping steeply toward the SE, and the hinges plunge moderately to the SW (Fig. 5h). The slump fold was re-folded into a rounded, open, NE–SW trending antiform (Am1 on Fig. 5b). It can also be outlined based on the thin dolomite layer, which covers the laminated intercalation. The thickness of this cover layer is changing on the limbs of the antiform. However, the dolomite layer, underlying the folded laminated intercalation, stays flat, and is not affected by the folding (Fig. 5b). We interpret these structures as early deformation features, slump folds (See Discussion).

Small neptunian dykes run down from the bituminous intercalations of the Hauptdolomit. The neptunian dykes are N–S-striking, and they are filled up with this dark-grey bituminous dolomite (Fig. 5i). The infillings suggest synsedimentary Triassic origin for the dykes and could be broadly coeval with the slump folds.

Based on dip data a 200 m-wide segment of the NE–SW trending Molnárkő anticline was recognized, although any marker beds can barely be followed along the entire quarry walls (Fig. 5a, c and g). Its hinge intersects the western edge of the southern wall (Fig. 5a), and the eastern edge of the northern wall (Fig. 5c), so the fold cut the entire quarry diagonally.

The anticline is rounded and gentle on the southern wall (Fig. 5a), whereas it is represented by a narrower open fold on the northern wall (Fig. 5c). There, the hinge is angular/sharp (Fig. 5c). The limbs are much steeper in the northern wall (Fig. 5c) than in the southern wall (Fig. 5a). Consequently, the interlimb angle of the anticline is decreasing northeastward. The hinge is dissected by small normal faults on the northern wall (Fm1 faults on Fig. 5c).

The northwestern limb is dissected by a small, apparently west-vergent thrust on the northern wall (Fm2 on Fig. 5c). The Molnárkő anticline is dissected by three NW–SE-striking steep faults (Fm3; Fm4; Fm5). The Fm3 fault is exposed on the southern wall (Fig. 5a); on the fault plane

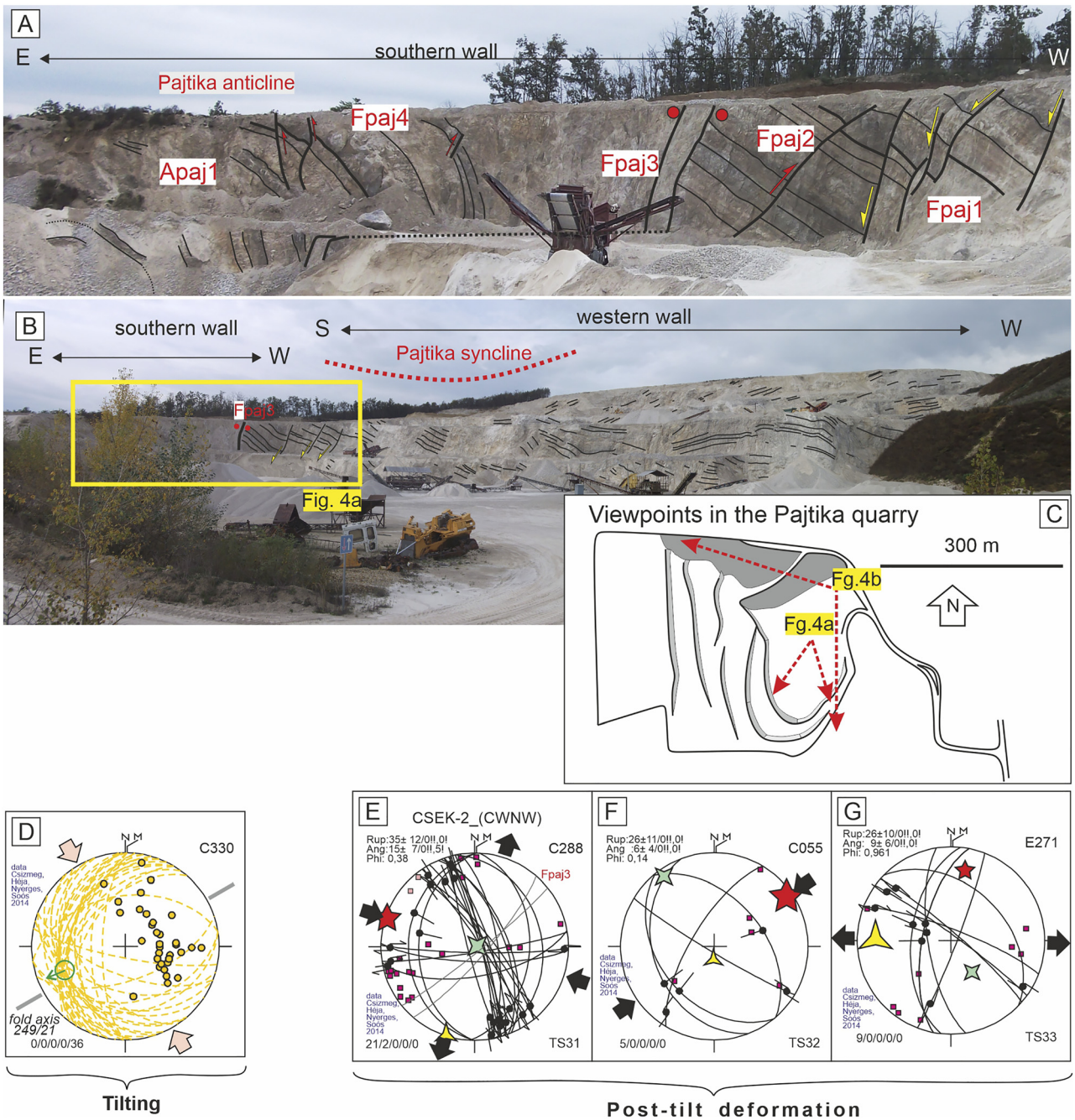

Fig. 4. Cserszegtomaj, Budai-hegy, Pajtika quarry: a) southern wall of the quarry; b) western wall of the quarry; c) map of the quarry with the view points of the photos; d) stereoplot of dip data; e-g) stereoplots of the post-tilt phases. For location of the outcrop, complete data set, legend for the stereoplots see Fig. 1c, Suppl. I. and Fig. 2c, respectively

oblique sinistral-inverse (Fig. 5e), and dextral-normal slickenlines are preserved (Fig. 5d). Steeper, oblique sinistral-inverse slickenlines (Fig. 5e) overprint sub-horizontal sinistral striae (Fig. 5f). These oblique slickenlines were possibly formed due to the reactivation of former NW–SE-striking faults. The middle steep fault (Fm4 on Fig. 5c) is NW–SE-striking, and shows apparent reverse offset, which may also indicate left-lateral movement. The Fm5 cuts the Fm1 set of faults; while it is parallel to Fm4, which is most probably also a sinistral fault.

Sub-horizontal sinistral slickenlines of the Fm3, together with a set of NEE–SSW-striking dextral faults, indicate a strike-slip type stress field with E–W compression and N–S extension (Fig. 5f). Oblique sinistral reverse faults measured on the fault plane of the Fm3, together with a few minor thrusts, suggest post-tilt NW–SE shortening (Fig. 5e); using overprinting criteria it is younger than the E–W compression. Albeit it is a weak argument, the relative chronology would indicate that the NW–SE folding was followed by E–W (post-tilt) shortening; then the NW–SE shortening

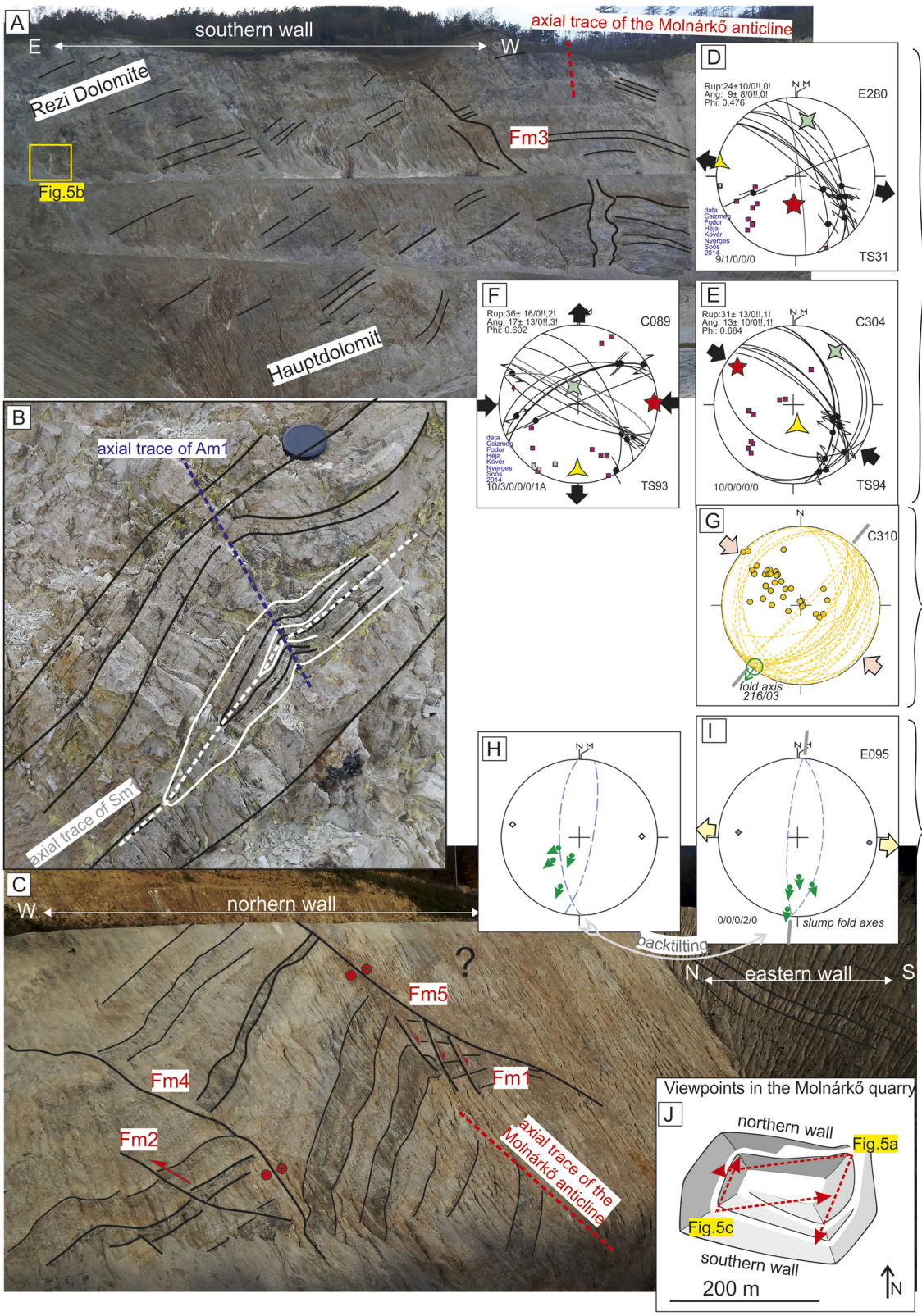

Fig. 5. Cserszegtomaj, Budai-hegy, Molnárkő quarry; (a) southern wall of the quarry; (b) slump fold in Rezi Dolomite (c) northern wall of the quarry d-f) stereoplots of the post-tilt phases (g) stereoplot of bedding dip data and calculated fold axis (h) recent orientation of early, pre-diagenetic structures (i) back-tilted orientation of early, pre-diagenetic structures (j) map of the quarry with the view points of the photos. For location of the outcrop, complete data set, legend for the stereoplots see Fig. 1c, Suppl. I. and Fig. 2c, respectively

reappeared. Oblique dextral normal slicken lines on the Fm3 fault plane developed due to post-tilt E–W extension (Fig. 5d).

Kőmell Cliff (Vony-03-04)

Rezi Dolomite is exposed at the Kőmell Cliff near Gyenesdiás (Fig. 1c). The lower part of the cliff is built up by massive dolomite in which the layering is not visible. The top of the cliff is made up of massive cherty dolomite, but up to 0.5 m-large blocks of laminated dolomite also occur in the massive dolomite matrix. On the highest part of the cliff, few meter-long individual blocks of cherty dolomite with well visible bedding occur. Albeit the dip azimuths of these beds are generally homogenously NNE, strongly different dip values are present. It may suggest that this part of the cliff is also built up by dolomite breccia, and the individual blocks of the well-bedded dolomite represent redeposited blocks (Fig. 6a and b). At the northeastern side of the cliff there is a WNW–ESE-trending asymmetric, overturned, closed anticline (Ak1 on Fig. 6c). The fold gradually smoothens upward and is covered by undisturbed beds.

Pilikán quarry (Vony-05)

Thin-bedded to laminated, dark-grey, bituminous dolomite (Rezi Fm) crops out in the Pilikán quarry (Fig. 1c). Triassic sedimentary breccia and NW–SE-striking small syn-sedimentary normal faults, suggesting NE–SW Late Triassic extension, were reported by Héja et al. (2018) in this quarry.

The most dominant structure of the quarry is the approximately 500 m-wide N–S-trending anticline with sharp hinge, the Pilikán anticline (Fig. 7a and c). The cross-section (Fig. 7c) clearly shows that the Pilikán anticline has a short, steeper eastern forelimb and a longer, gently dipping western backlimb. The western limb of the anticline is dissected by a tilted conjugate thrust pair on the northern wall (Fig. 7d and e). Tilt-test of measured data suggests that this conjugate thrust plane preceded the formation of the Pilikán anticline (Fig. 7f and g). The back-tilted thrust pair suggests WNW–ESE shortening (Fig. 7g). We measured several shallow-dipping fault planes without striae. Based on conjugate fault pairs these structures can be interpreted as two distinct phases; one phase of post-tilt thrust faults marked by the same E–W shortening as the anticline (Fig. 7h), and another contractional phase with NE–SW shortening (Fig. 7i).

Gyenesdiás quarries

The Gyenesdiás quarries expose/preserved one of the most complex deformation histories, where almost all deformation phases left their traces (Figs 8–10). The most prominent structure is the NNW–SSE-trending Gyenesdiás anticline, which extends into all of the three quarries (Figs 1c and 8), exposing different parts of this anticline; the quarries are described in the following sub-chapters one after another.

Gyenesdiás, eastern quarry (Vony-20-21). A relatively thick succession of steeply ENE-dipping, highly fractured dolomite beds crops out in this quarry. The dolomite is frequently friable/powdered near bedding surfaces. In the western wall thick beds of Hauptdolomit occur, whereas the southern wall exposes the alternation of thin-bedded, laminated, dark grey bituminous dolomite and thick-bedded dolomite (Rezi Formation) (Fig. 9a, b and d). Slump folds and tilted conjugate normal fault pairs in the southern wall indicate the presence of pre-folding deformations in this quarry (Héja et al., 2018); tilt test clearly indicates the pre-folding origin of these fractures (Fig. 10w and t).

On the eastern part of the southern wall a few meters-wide pop-up structure occurs (Fig. 9a), which is bordered by conjugate thrusts (Fgy1 fault set), with a few tens of centimeter offset. The pop-up anticline is more remarkable in the upper level, whereas it gradually disappears downward (Fig. 9a).

We measured several sub-vertical fault planes with steeply plunging slickenlines (Fig. 10y). Back-tilting of these faults with the actual steep dip suggests that these faults are pre-folding thrusts (Fig. 10s). Post-folding strike-slip faults with the same maximal stress axes as for the thrusts can represent a later event within the same contractional deformation (Fig. 10o).

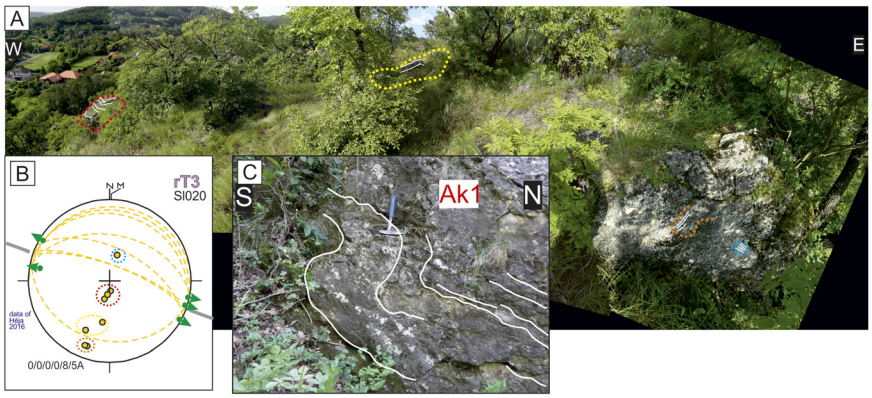

Fig. 6. Kőmell Cliff (a) individual crags at top of the Kőmell Cliff show significantly different dips (b) stereoplot of bedding dip data; dashed circles indicate different blocks; (c) slump fold in the northern side of the cliff. For location of the outcrop, complete data set, legend for the stereoplots see Fig. 1c, Suppl. I. and Fig. 2c, respectively

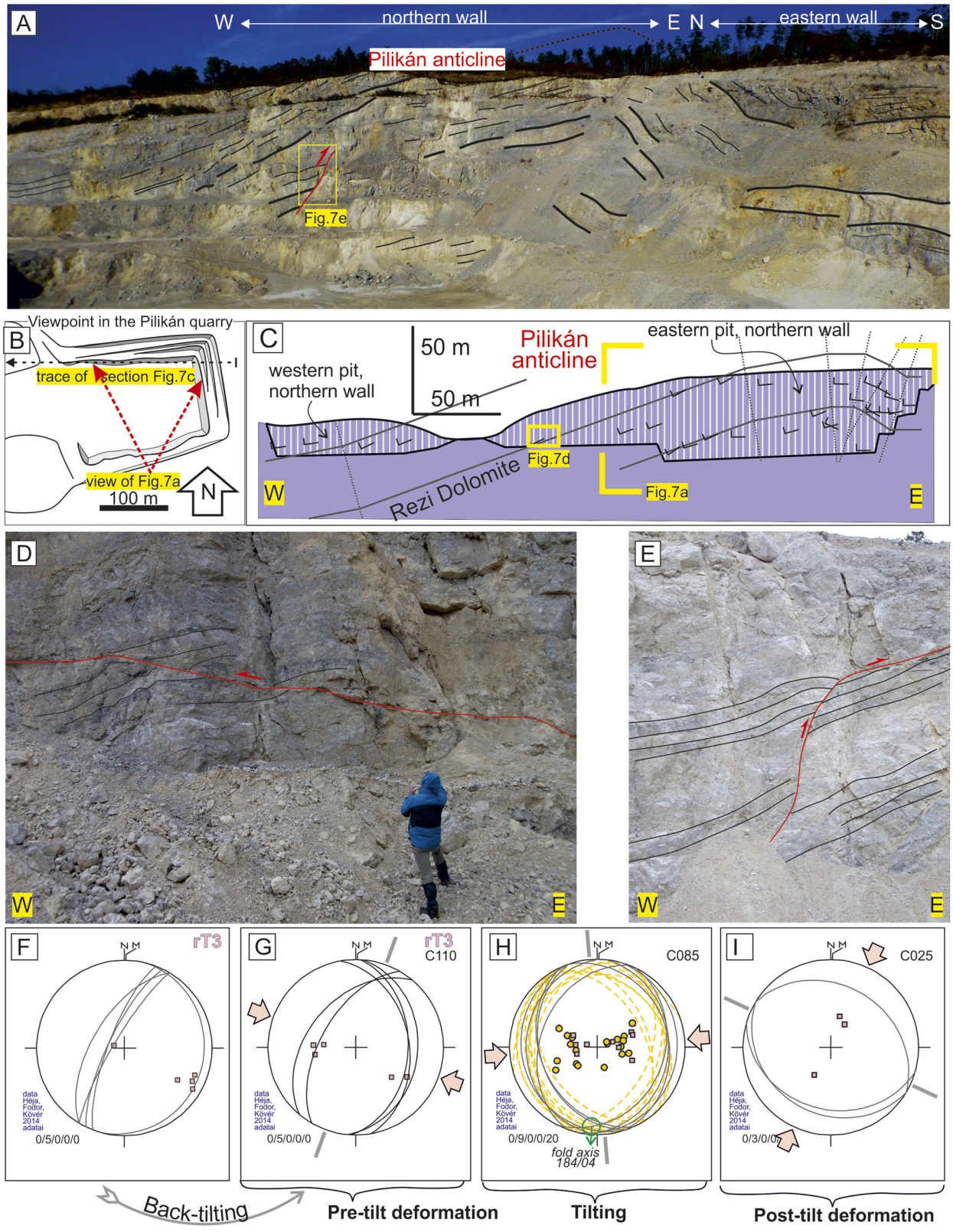

Fig. 7. Structures of the Pilikán quarry (Keszthely): a) Pilikán anticline on the northern wall; b) map of the quarry with the view points of the photos; c) cross section view of the Pilikán anticline with the measured dip data, striped area indicates the extent of the quarry; (d, e) tilted conjugate set of thrust planes; (f, g) stereoplots of the conjugate thrust planes in present day, and back-tilted position; h) stereoplot of beddings and N–S-striking conjugate thrusts; i) post-tilt conjugate thrusts. For location of the outcrop, complete data set, legend for the stereoplots see Fig. 1c, Suppl. I. and Fig. 2c, respectively

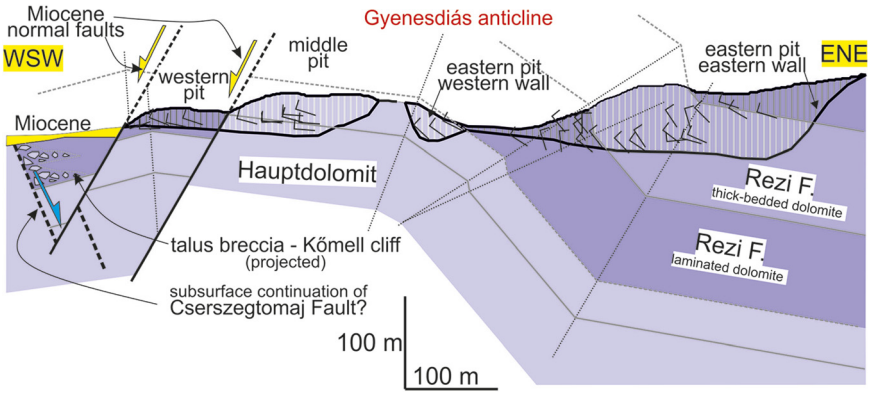

Fig. 8. Cross-section across the three Gyenesdiás quarries; striped areas indicate the extent of the quarry; (Sites Vony-01-02, -20-21)

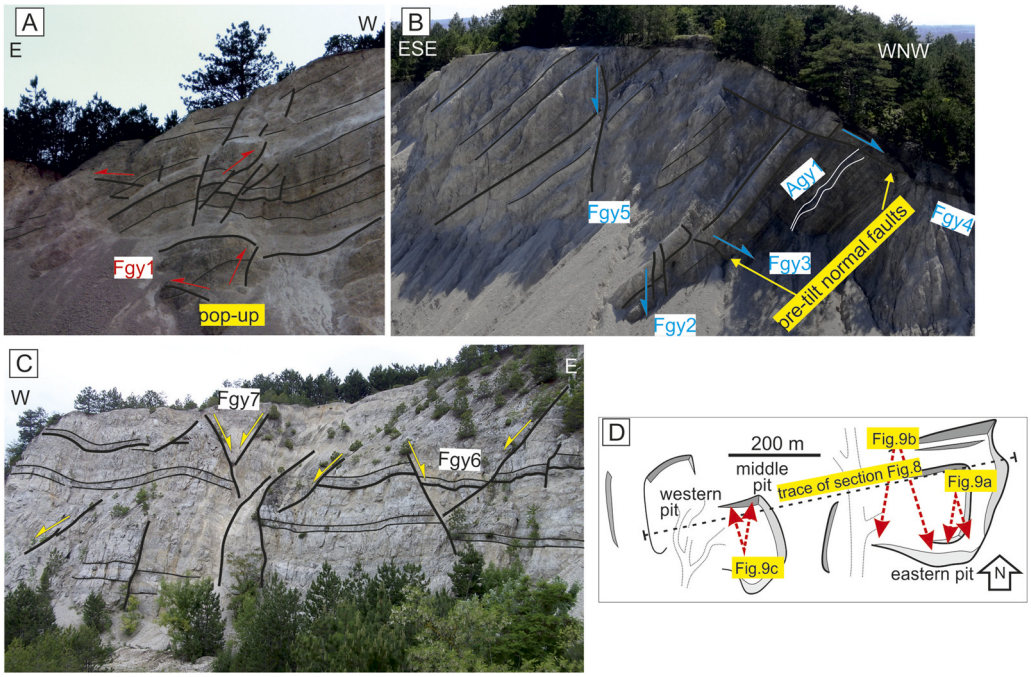

Fig. 9. Gyenesdiás quarries (a) pop-up structure on the southern wall of the eastern quarry (b) tilted normal faults on the southern wall of the eastern quarry (c) conjugate normal faults in the middle quarry (d) location map of the quarries. For location of the outcrop, complete data set see Fig. 1c, Suppl. I. and Fig. 2c, respectively

Several post-tilt normal faults occur in this quarry. A set of SW-dipping fault planes dissect the tilted dolomite beds with normal offset. Although there were no slickenlines on these planes, we considered these structures as normal faults, formed in a NE–SW extensional stress-field (Fig. 10k). Normal slickenlines on NNW–SSE striking conjugate normal fault pairs suggest perpendicular ENE–WSW extension (Fig. 10j). Oblique dextral-normal slip of the NW-striking faults seems to indicate their reactivation by an E–W extension (Fig. 10j) but the separation of these two extensional directions is difficult, because the complete data set still shows good fit. Some NNE-striking faults may be neoformed structures better corresponding to the new extensional direction (Fig. 10d).

Gyenesdiás middle quarry (Vony-01). In this quarry, beds of the Hauptdolomit are sub-horizontal (dipping gently towards NNE). When considering the whole set of dip data in all Gyenesdiás outcrop, the gentle dip fit to a folded structure with ENE–WSW shortening (Fig. 10p).

WNW–ESE-oriented compression was calculated based on NNW–SSE-striking sinistral and E–W-striking dextral strike-slip faults (Fig. 10x). Two oppositely dipping thrusts with oblique slip fit into this stress field (Fig. 10x). Due to the moderate dip of the beds, the tilt test (Fig. 10r) does not give an unequivocal result for strike-slip faults; they could be either pre- or post-tilt fractures. On the other hand, the back-tilting of the two thrusts gives a better geometry while they bear nice dip-slip striae in the original position

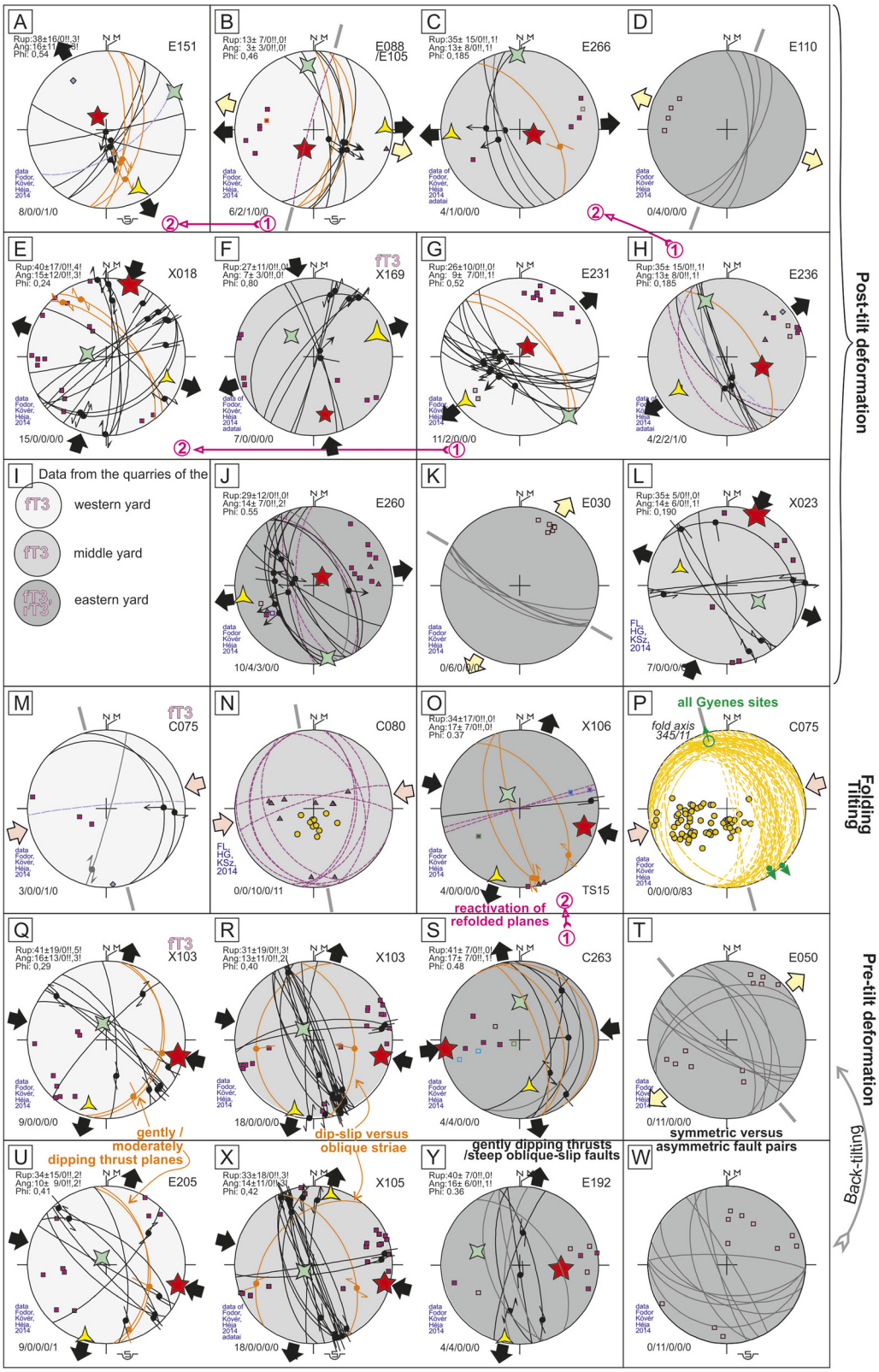

Fig. 10. Stereoplots from the quarries of Gyenesdiás (Vony-01-02, -20-21). See Fig. 2c for the legend of stereoplots and additional legend on Fig. 10i. Faults that suffered reactivation appear on more than one stereoplot. These faults are highlighted by orange color. For location of the outcrop, complete data set, legend for the stereoplots see Fig. 1c, Suppl. I. and Fig. 2c, respectively

(Fig. 10r). A set of gently-dipping conjugate joints can also be interpreted as conjugate Mohr-pairs associated to E–W-shortening (Fig. 10n); these fractures could form either before or after the modest tilting.

We also measured some NNW–SSE-striking dextral and E–W-striking sinistral faults (Fig. 10l). These faults cannot be interpreted as simple strike-slip conjugate pairs due to their large obtuse angle. In our interpretation these fault-slip data represent the reactivation of a pre-existing conjugate fault system (Fig. 10x) due to NNE–SSW-shortening and perpendicular tension (Fig. 10l). NNE-trending sinistral strike-slip faults and some steep normal faults could belong to a closely N–S compression and perpendicular extension (Fig. 10f, for complex interpretation of this stress state, see Suppl. I.).

In the quarry wall, beds are dissected by several conjugate normal faults (Fgy6-7 on Fig. 9c), which belong to two stress states. At a smaller scale, steeply plunging normal striae occur on some of the SW-dipping steep fault planes, which possibly developed in a NE–SW extensional stress-field, together with a few SW-dipping joints and calcite veins (Fig. 10h). We measured a few conjugate normal faults, which fit to an E–W extension (Fig. 10c); one oblique normal slip can indicate the reactivation of former normal faults of the NE–SW extension by the younger E–W extension (orange line on Fig. 10h and c).

Gyenesdiás, western quarry (Vony-02). This outcrop is situated in the western vicinity of the previously described quarry (Figs 8 and 9d). It is built up by thin-bedded, laminated, dark grey, gently dipping Rezi Dolomite. The gentle WNW dip values represent the western limb of the Gyenesdiás anticline. Pre-orogenic normal faults with a few tens of cm offset and a very gentle flexure above the upper fault tips were attributed to Triassic deformation (Héja et al., 2018).

We measured several thrusts dipping gently towards to the east. These structures suggest an almost E–W compression, together with NW–SE-striking sinistral strike-slip faults (Fig. 10u and m); part of the faults could be pre-tilt in origin (Fig. 10q). We found several SSW-dipping dextral normal faults with oblique slickenlines, and a few SW-dipping normal faults (Fig. 10g). These structures suggest NE–SW extension (Fig. 10g). The WNW–ESE-striking oblique slip faults (Fig. 10g) might have been reactivated along pre-existing normal faults, which could indicate the presence of an earlier NNE–SSW extensional phase. NE–SW-striking sinistral faults and N–S-striking dextral faults represent conjugate pairs of strike-slip faults, which show NNE–SSW compression and perpendicular WNW–ESE tension (Fig. 10e). Oblique dextral reverse slickenlines on moderately NE-dipping fault planes fit into this stress-field. It is possible that the NE-dipping fault planes originally represented the antithetic pairs of the SW-dipping normal faults, and the recently-observed oblique slickenlines are the result of oblique reactivation (orange lines on Fig. 10e and g). This presumption gives a relative order: the NE–SW extension could have been post-dated by the NNE–SSW transpression.

We observed two generations of slickenlines on the east-dipping fault planes. The east-plunging dip-slip slickenlines suggest E–W extension (Fig. 10b), whereas the oblique dextral normal slickenlines can be interpreted as the dextral-normal reactivation of these E-dipping planes by a NW–SE extension (Fig. 10a).

Further outcrops near Gyenesdiás (Gyen-01-04; Bf-39)

We measured a few strike-slip and oblique-slip normal faults, and several gently-dipping joints and faults in Hauptdolomit along a forest road north of Gyenesdiás (Faludi erdő, site Gyen-01-04). NW–SE-striking gently dipping faults and joints outline conjugate thrust pairs. These data together with a few N–S-striking dextral faults and one N-dipping sinistral fault suggest NE–SW-shortening (Suppl. I.).

Vadlánylik (site Bf-39), which is situated south of the eastern pit of the Gyenesdiás quarries, is a cave which is formed in Miocene breccia, which consists of redeposited dolomite clasts. We found NNE–SSW-striking conjugate normal fault pairs and deformation bands in this natural outcrop (Suppl. I).

Vonyarcvashegy, "Keresztes" quarry (Vony-22)

Sub-horizontal beds of the Hauptdolomit are exposed in this small quarry (Fig. 1c). The flat-lying layers make it pointless to apply tilt test on the measured faults. We classified the observed structures into four stress-fields. The E–W-striking sinistral faults developed due to NE–SW-shortening and NW–SE tension (Fig. 11d). The N- and S-dipping conjugate normal fault pairs represent another population of faults, which developed in an N–S extensional stress field (Fig. 11c). The ENE-plunging striae on the NE-dipping fault planes suggest NE–SW extension (Fig. 11b). These oblique slip faults are possibly reactivated NNE-dipping earlier normal faults. An additional E–W-striking fault can be classified into this phase, with steeply plunging dextral slickenlines (Fig. 11b). This fault possibly represents the reactivation of one of the above-described sinistral strike-slip faults (Fig. 11d and b). NW-dipping normal faults developed due to NW–SE tension, together with two steep south-dipping sinistral normal faults. These latter oblique-slip faults possibly represent the reactivation of the previously-formed south-dipping normal faults (Fig. 11c and a).

Vonyarcvashegy, "Felső-hegy" quarries (Vony-35, -44)

The Hauptdolomit Fm is exposed in these two small, abandoned quarries (Fig. 1c). The bedding dips mostly toward the NE. Late Triassic syn-sedimentary normal faults and neptunian dykes were described from the southern quarry (Vony-35) by Héja et al. (2018). Few tens of cm-deep neptunian dykes cut across the thick light grey dolomite beds, and they are filled up by dark bituminous dolomite. These neptunian dykes show various strikes in the southern quarry (Fig. 12j), but they are mostly NW–SE-striking in the

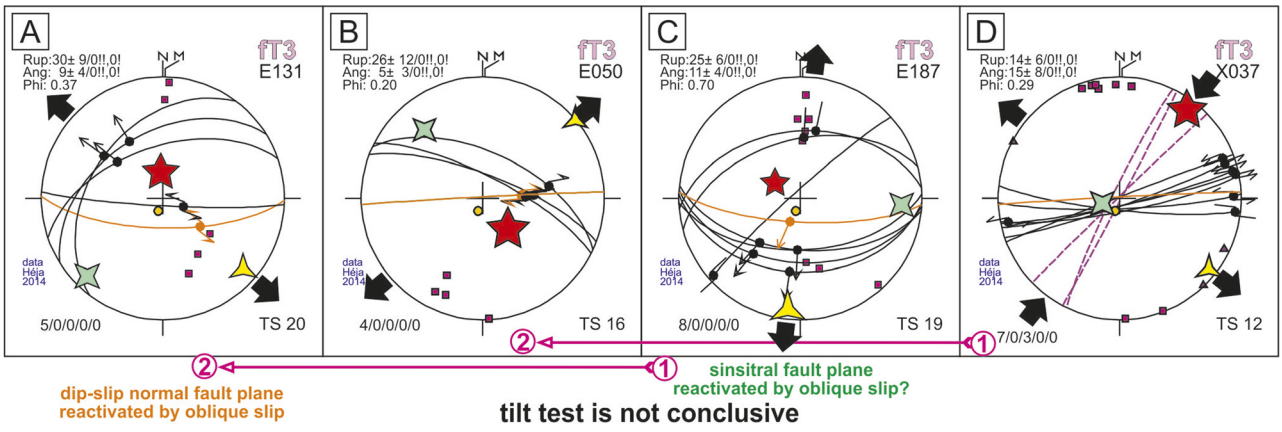

Fig. 11. Stereoplots from the Vonyarcvashegy, "Keresztes" quarry (site Vony-22). Faults that suffered reactivation appear on more than one stereoplot. These faults are highlighted by orange color. For location of the outcrop, complete data set, legend for the stereoplots see Fig. 1c, Suppl. I. and Fig. 2c, respectively

northern quarry (Fig. 12k, site Vony-44). We measured several joints in the southern quarry, which can be considered as pre-folding extensional conjugate fracture pairs, based on tilt-test (Fig. 12i and f). Dip variations outline a gentle fold (Fig. 12e) which marks the Cretaceous folding.

We measured several horizontal striae on E–W-striking sub-vertical faults, with poorly constrained sinistral sense in the southern quarry (Vony-35). These fault-slip data show NE–SW-shortening and perpendicular, NW–SE extension (Fig. 12d). Other faults dipping towards the NE and SW form ideal conjugate normal fault pairs, which developed in a NE–SW extensional stress field (Fig. 12c). WNW–ESE-striking sinistral faults and NE–SW-striking normal faults observed in the southern quarry suggest a NW–SE extensional stress-field (Fig. 12a). We measured oblique sinistral-reverse slickenlines on a SE-dipping fault plane in the northern quarry (Fig. 12b).

Balatongyörök quarry and road cut (Bgyö-01, Bgyö-05)

Steeply N-dipping Hauptdolomit is exposed in this quarry (Figs. 1c, 13c and d). Microbialitic interbeds occur frequently between thick massive dolomite beds. These dolomite interbeds are often friable/powdered; in this case, the original microbial laminae cannot be recognized. The massive dolomite beds in the vicinity of the friable zones are strongly fractured. Several SW-dipping thrusts (Fb1-4) cross-cut the tilted beds (Fig. 13c). These thrusts seem to root in layer-parallel friable dolomite zones, and they do not cross-cut all the friable dolomite layers. The separations of these thrusts are less than a meter (Fig. 13c). We could measure only the Fb1 thrust, which dips toward the SW (Fig. 13d).

A thick dolomite bed is exposed east of this quarry, along the highway (Site Bgyö-05). NW–SE-striking sinistral strike-slip faults were measured in this site. While tilt test shows that striae are more horizontal in back-tilted than present-day position, the faults are considered as pre-tilt in origin (Fig. 13a and b). Based on these faults an E–W compression can be calculated, which is in line of other stress/shortening data of the surroundings.

Szent Miklós spring, ravine (II-31)

This outcrop is located in the eastern KH, near the Ederics platform (Fig. 1c). East of the Szent Miklós spring the Carnian Veszprém Marl Formation is exposed in a small ravine (Csillag et al., 1983, 1995). The deformed beds consist of well-bedded marly limestone and thin-layered to laminated marl. A meter-wide tight anticline is outlined in the thin-layered – laminated beds. The eastern limb of the anticline is vertical or overturned, and it is crosscut by a small reverse shear zone with a few centimeters of off-set (Fig. 14a and c).

Immediately east of this fold, the beds dip moderately westward (out of the photo), similarly like in a western limb of the anticline (Fig. 14a). This suggests that the eastern vertical/overturned limb of the anticline is turning back into a syncline directly east of the anticline (right to the photo of Fig. 14a). Consequently, the anticline has a longer western, and a shorter eastern, limb, and the axial plane of the fold is dipping westward (Fig. 14a and c).

We measured several joints in this outcrop; normal shear was attributed to a small group of E–W-striking joints on the back-tilted stereoplot, which suggests N–S extension prior to folding (Fig. 14b). The eastern limb of the anticline is dissected by several NNE–SSW-striking joints, which form post-tilt extensional conjugate pairs (Fig. 14d).

Lesencefalu quarry (Lese-01)

Poorly preserved friable dolomite and the strongly cemented beds of the overlying Upper Miocene conglomerate are exposed in this small quarry near Lesencefalu (Fig. 1c). The rounded or sub-angular clasts of the conglomerate consist of redeposited, locally sourced dolomite (Fig. 15a). This sediment belongs to the Diás Member of the Békés Gravel Fm, of abrasional origin (Budai et al., 1999a, b). The measured dips of the Miocene beds outline a very gentle E–W-trending

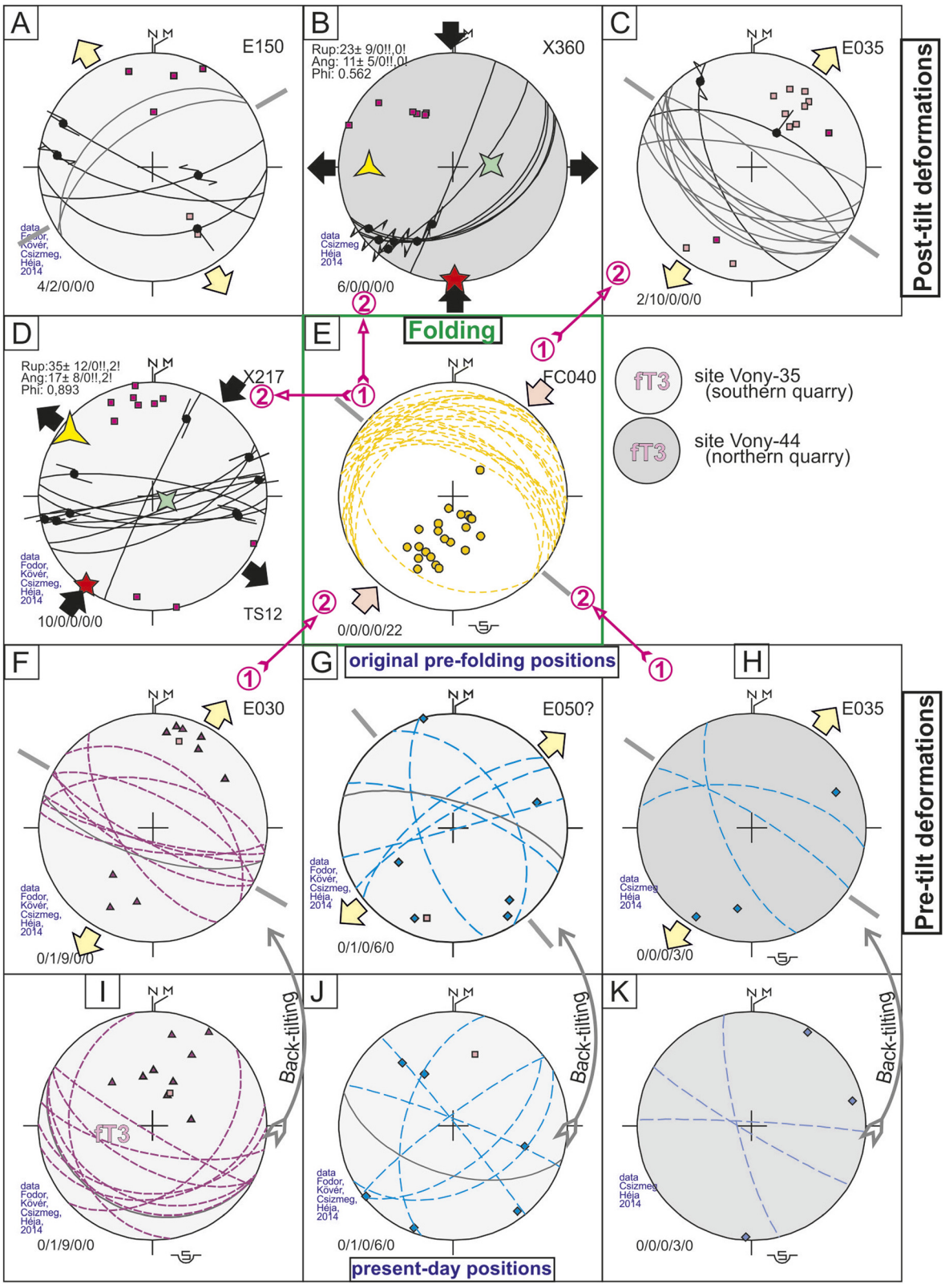

Fig. 12. Stereoplots of measured data from Vonyarcvashegy, Felső-hegy quarries (sites Vony-35 (light grey) and Vony-44 darker grey). Note relative chronology with respect to the folding phase. For location of the outcrop, complete data set, legend for the stereoplots see Fig. 1c, Suppl. I. and Fig. 2c, respectively

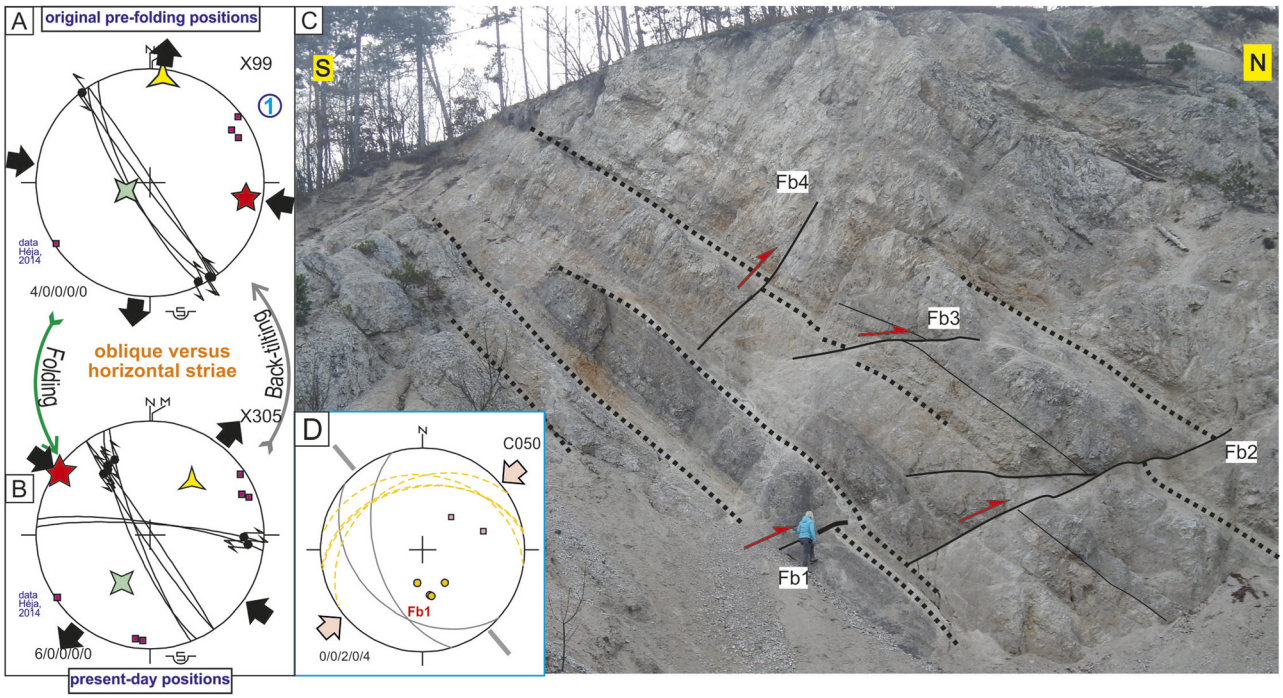

Fig. 13. a) Stereoplot of back-tilted strike-slip faults of the Bgyö-05 site; b) stereoplot of the oblique strike-slip faults of the Bgyö-01 and Bgyö-05 sites (present-day position); c) Structures of the Balatongyörök quarry (BGyö-01). d) Stereoplot of Fb1 thrust and bedding planes. For location of the outcrop, complete data set, legend for the stereoplots see Fig. 1c, Suppl. I. and Fig. 2c, respectively

anticline (Fig. 15c), which can have a tectonic origin or one related to the depositional geometry (e.g., a small fan). The conglomerate beds are dissected by a ESE-dipping normal fault (Fig. 15a and b). A monocline occurs above the tip point of the fault along the upper surface of the layer (Fig. 15a and b). This surface shows continuous deformations and is not displaced by a discrete fault; this suggest that this flexure came into being before or during the complete diagenesis of the deformed Miocene bed and is considered as a syn-diaganetic feature/element.

Várvölgy, Csetény quarry (Varv-01)

Southwestward-dipping beds of the Hauptdolomit are exposed in this quarry (Figs 1c and 16a). We measured a set of moderately NE-dipping fault planes, with oblique dextral normal slickenlines, in this quarry (Fig. 16c). These fault-slip data can be interpreted as oblique reactivation of a NW–SE-striking normal faults (Fig. 16b) in a transtensional stress-field, which can be characterized by N–S-shortening and E–W extension (Fig. 16c).

Road cuts between the Vár Valley and the Büdöskút (Vony-06-10)

Beds of the Hauptdolomit Fm are exposed along the road cuts of the forest road between the Vár Valley and the Büdöskút (Fig. 1c). Due to their small size, we merged the structural data of several outcrops. The dip data of the beds outline an N–S-trending fold (Fig. 17h). Some of the joints can be classified as pre-tilt conjugate strike-slip and reverse faults (Fig. 17j). We measured several gently west-dipping fractures, which may represent minor post-tilt thrusts (Fig. 17g). Another set of low-angle fractures can be explained by NW–SW shortening (Fig. 17e). A few oblique sinistral-normal faults developed due to E–W extension (Fig. 17b). Another set of joints and faults outline nice post-tilt extensional conjugate pairs, showing NNW–SSE extension (Fig. 17a). A single relative chronological datum suggests that this latter stress state preceded the E–W extension.

Road cuts between Büdöskút and Balatongyörök (Vony-11-15, -29, -32)

The beds of the Hauptdolomit and Rezi Dolomite are exposed along the forest road-cuts between Büdöskút and Balatongyörök (Fig. 1c). As in the previous paragraph, we merged the structural data of several small outcrops in this section. At sites Von-15 and -32 small folds can be interpreted as slump folds (Fig. 17l). Conjugate pairs of normal faults have a vertical symmetry plane after back-tilting, suggesting that they formed before any tilt of the layers (Fig. 17k and n). These fractures are interpreted as the result of pre-folding NE–SW extension and could represent the oldest tectonic deformation. The measured dip data outline an NNW–SSE-trending fold (Fig. 17i). NW–SE-striking sinistral strike-slip faults together with several N–S-striking, gently dipping conjugate pairs of joints suggest a transpressional stress field where the direction of shortening is WNW–ESE (Fig. 17f).

We classified a few conjugate normal faults into a post-tilt NE–SW extensional stress field (Fig. 17d). Another set of N–S-striking joints possibly formed due to E–W extension. A steep SW-dipping dextral fault can be enrolled into this

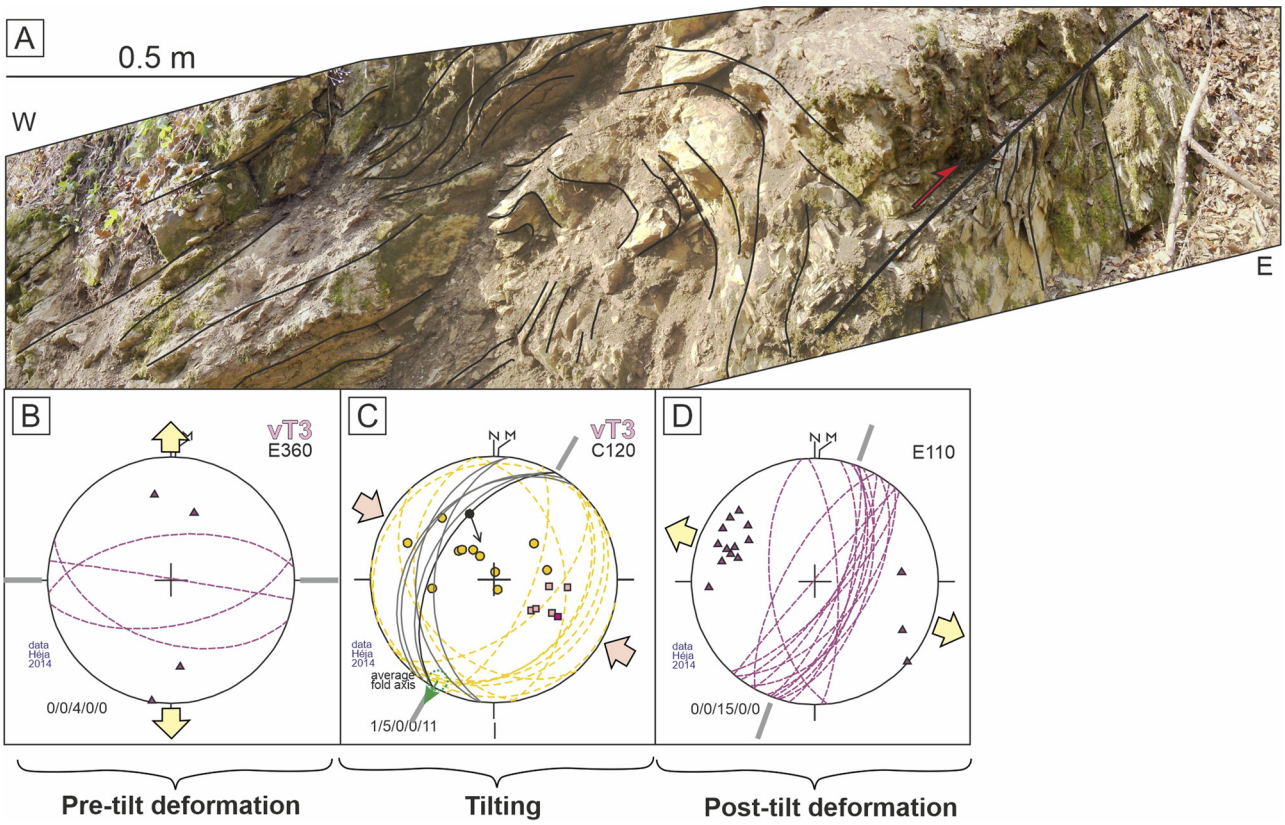

Fig. 14. a) Folded Carnian Veszprém Marl near Szent Miklós spring, eastern Keszthely Hills; b) NNE–SSW-trending anticline is outlined on the stereoplot of dips. For location of the outcrop, complete data set, legend for the stereoplots see Fig. 1c, Suppl. I. and Fig. 2c, respectively

phase and this fault can represent the strike-slip reactivation of a former normal fault (Fig. 17c).

Outcrops north of Rezi, Hosszú Valley and Púpos Hill (Bf-33-37, Bf-38)

Natural outcrops in the Hosszú Valley and on the western slope of the Púpos Hill (Bence et al., 1982) reveal important information on the Late Miocene (Pannonian) deformation (Figs 1c and 18a). The long and narrow valley trends NW–SE and the Pannonian outcrops are near the bottom of the valley (Bence et al., 1982; Budai et al., 1999b) (Fig. 18a). This geometry suggests that the narrow Pannonian belt is bounded on both sides by normal faults (Fig. 18e). In fact, the southwestern fault is almost exposed in the valley bottom between the Triassic and Pannonian, but the strike deviates toward WNW–ESE. The northeastern fault continues southward, and forms the eastern boundary of the Rezi Graben. All these faults were schematically illustrated in Csillag and Nádor (1997). Southwest of Hosszú Hill other faults can be postulated on the basis of the disposition of the Pannonian and Triassic formations (the latter in higher position), and fault strike varies between NNE–SSW and NNW–SSE.

The sites near the valley bottom (Bf-33-37) show variable clastic sediments, ranging from silt, sand, and clay, with occasional pebbles, lignite seams and plant remnants (observation of K. Sebe, pers. comm.). These sediments are cut by joints, but a few fractured pebbles were also measured.

Site Bf-38 (Fig. 18a) is composed of dolomite breccia of variable grain size and roundness (Fig. 18b–d). The largest blocks can reach several meters in size, and generally represent flat fragments of some beds. Some rounded pebbles are also present, probably deriving from abrasion. The matrix is composed of 1 mm to few cm-diameter angular dolomite clasts. A crude bedding can be delineated by grain size variations and strings of coarser clast lag. The largest, outsized clasts seem to show a coarsening upward tendency. The layers can be assigned to the Diás Formation, which frequently occurs along faults in the KH (Csillag and Nádor, 1997; Budai et al., 1999b) and in other TR sites as well (Csillag et al., 2004).

The clasts show signs of brittle deformation; these include fractured clasts (sometimes with several fractures within single clasts), slightly displaced clast fragments, and fissures filled with the matrix (Fig. 18d). These features indicate active deformation during the fracturing of the clasts, probably already embedded in the soft and water-saturated matrix. Seismic shocks transmitted by the matrix induced fracturing in the rigid clasts. Such fractured pebbles indicate coeval deformation in other areas as well (Swierczewska et al., 2007). A few clast surfaces bear striation, indicating slip, probably during the break-off of the clasts. All these features may suggest an origin of the breccia as fault-bounded talus cone or apron. The sudden pinching out of the breccia body toward the finer-grained clastics also point to a localized occurrence, potentially along an active fault (Fig. 18e).

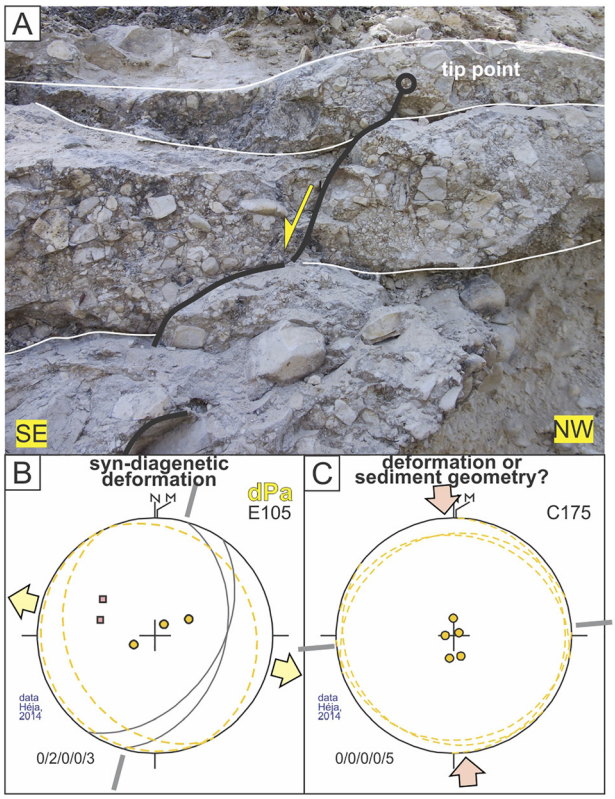

Fig. 15. Structures of the Lesencefalu quarry (Lese-01). For location of the outcrop, complete data set, legend for the stereoplots see Fig. 1c, Suppl. I. and Fig. 2c, respectively

The fractures are organized into two sets striking NW–SE and NE–SW but do not bear direct kinematic indices. Judging from the variable strike of the map-scale faults, and fault-slip data from other sites, these fractures might have formed in one stress field, characterized by ~N–S compression and ~E–W tension (Fig. 18g). This is similar to the fracture pattern of several other sites presented in previous sub-chapters (e.g., Figs 10b–d, 14d, 15, 16c and 17b, c, Suppl. I.) and observed already during the geologic mapping (Dudko in Budai et al., 1999a). The talus-cone breccia, the fractured, displaced or striated clasts can point to deformation just before the formation and just after the deposition of the clasts, so they can be Late Miocene in age.

Natural outcrops in the north eastern part of the Keszthely Hills (II-26, II-33-34, II-35-44, II-46, II-47-51)

We measured several joints and faults (Suppl. I.) on the natural outcrops and cliffs of Sédvölgy Dolomite and Hauptdolomit in the northeastern part of the KH (for location see. Fig.1c and Table. 1). Back-tilted faults and joints outline conjugate pairs of strike-slip faults and thrust, that suggest E–W (site II-26) and NW–SE (sites II-33-34) shortening prior to the tilting of the Triassic beds (Suppl. I.).

NE–SW-striking conjugate pairs of joints suggest post-tilt NW–SE shortening in the sites II-47-51 (Suppl. I.). We measured several NW–SE-striking, gently dipping joints and faults, which form post-tilt conjugate pairs of thrusts, suggesting NE–SW shortening (sites II-26, II-33-34, II-46). A few data suggest even N–S shortening (sites II-46, II-47-51). Moderately dipping joints form NE–SW (sites II-33-44, II47-51) and NW–SE (sites II35-44)-striking conjugate pairs, which suggest the presence of post-tilt NW–SE and NE–SW extensional phases (Suppl. I.).

DISCUSSION – DEFORMATION HISTORY: INTERPRETATION OF STRUCTURAL PATTERN, STRESS FIELD

We classified the previously described structural data into eight deformation phases. Except for Late Triassic and Late Miocene syn-sedimentary structures the timing of these phases

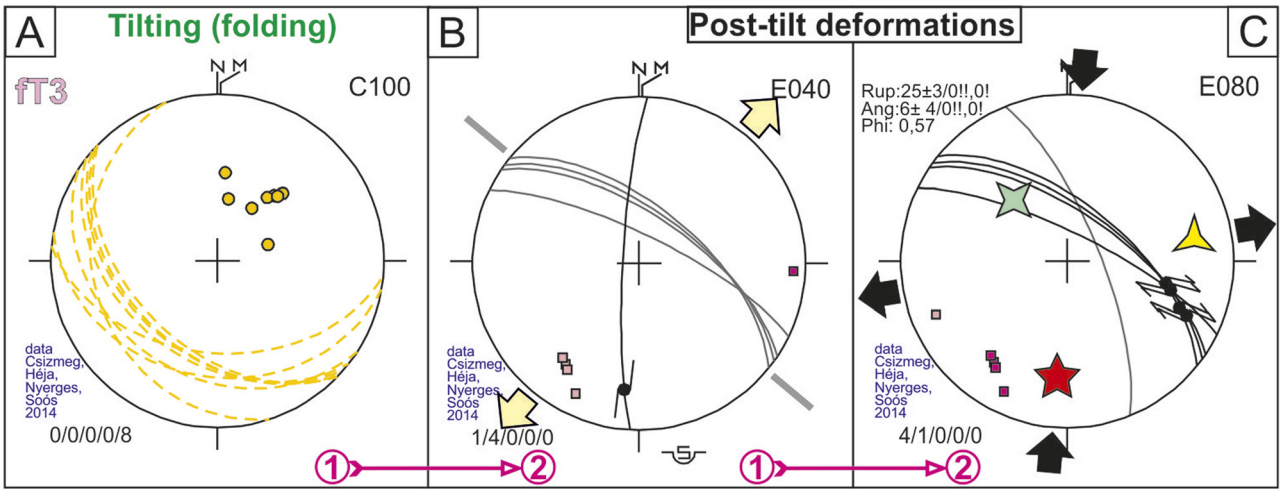

Fig. 16. Stereoplots of the Vár Valley Csetény quarry (Varv-1). Note relative chronology between deformation phases. For location of the outcrop, complete data set, legend for the stereoplots see Fig. 1c, Suppl. I. and Fig. 2c, respectively

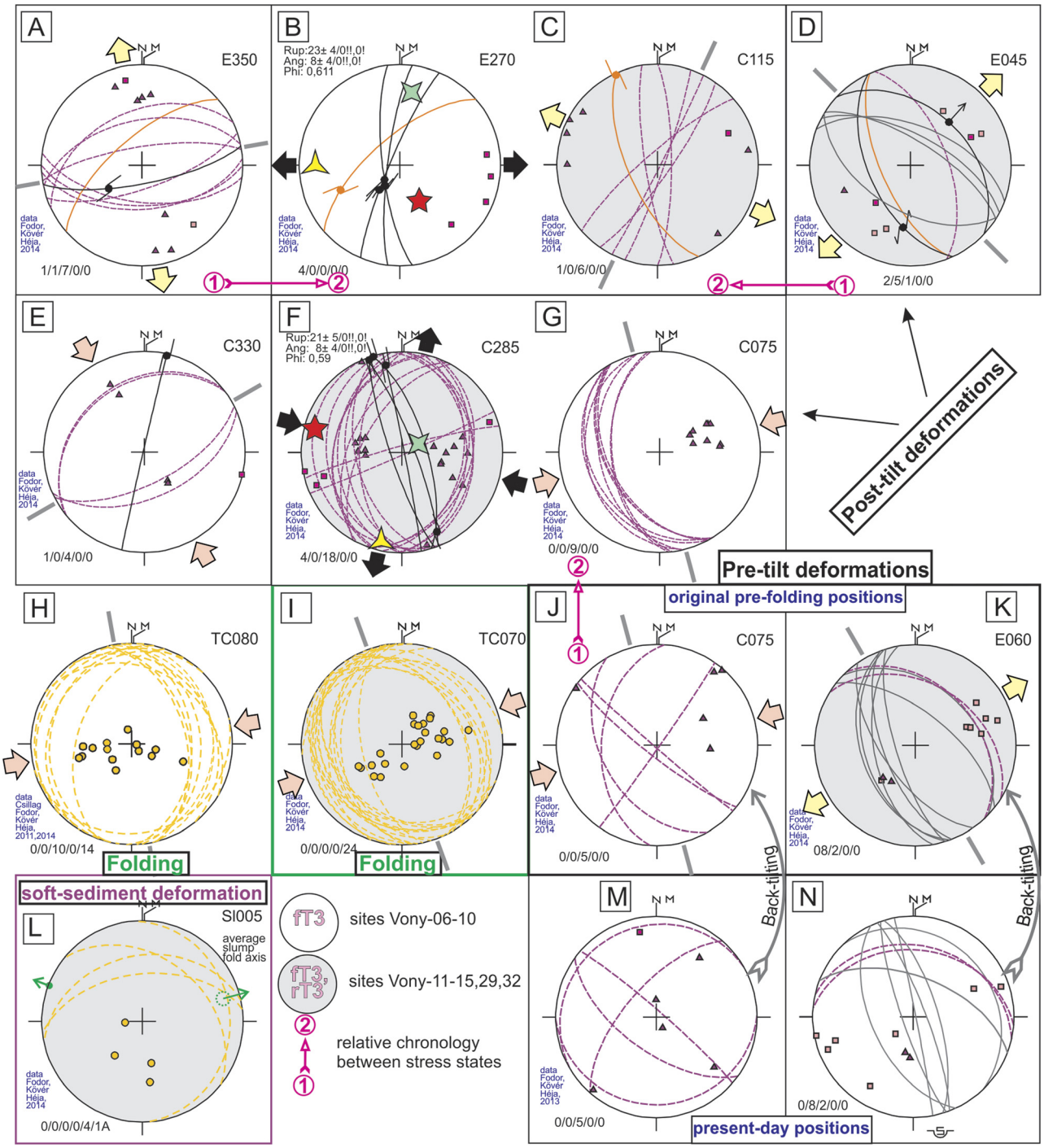

Fig. 17. Stereoplots of outcrops along the road from the Vár Valley to Balatongyörök and near Büdöskút (sites Vony-06-15, -29, -32). For location of the outcrop, complete data set, legend for the stereoplots see Fig. 1c, Suppl. I. and Fig. 2c, respectively

is problematic due to the reduced stratigraphy of the Keszthely Hills (KH). We determined the relative order of the deformation phases based on different types of crosscutting relationships (description in Methodology). The absolute ages of the deformation phases have been determined by the thorough comparison with other structural studies made in different parts of the TR, where a more complete stratigraphic succession is preserved. The reconstruction of the deformation history helped us to determine the age and kinematics of major map-view structures of the KH.

Late Triassic to Early Cretaceous (?) extension - D1 and D2 phases

Mesoscale structures of the D1 and D2 phases. Structures of the D1 phase correspond to Late Triassic extensional deformations (Suppl. I.). We classified all the syn-sedimentary normal faults and neptunian dykes into this phase, which were measured in Triassic rocks. Slump folds and sedimentary breccia bodies of the Rezi Dolomite also reflect,

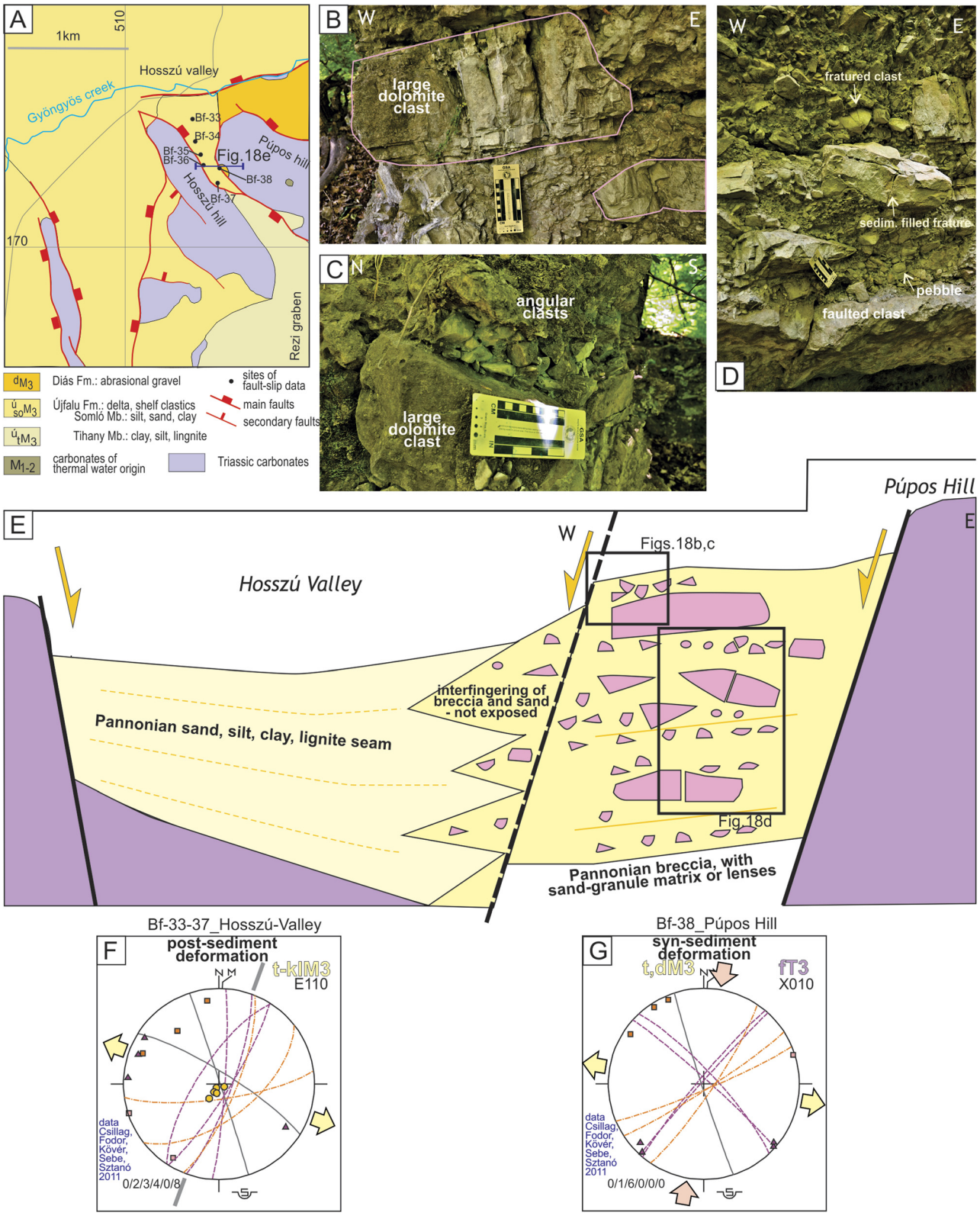

Fig. 18. Structural situation around the Hosszú Valley and Púpos Hill, Rezi. a) geologic map showing the Pannonian Formations and the topography below the uncolored Triassic dolomite. b, c) Outsized dolomite clast within angular clasts. d) fractured clasts, sediment-filled fractures within the Pannonian breccia. e) schematic cross section showing the main relationship between formations and graben bounding faults. f, g) stereograms for the sites in the valley and near the Púpos Hill

albeit indirectly, the effect of this extensional phase (Csillag et al., 1995; Héja et al., 2018). Tilted conjugate normal fault pairs represent the second phase (D2), which are post-sedimentary structures, but which preceded the Cretaceous folding. The most important structures of these early phases have been documented by Héja et al. (2018), but some of the features observed in the outcrops of the KH appear in this work (Vony-03,04,11, 44).

The measured neptunian dykes show a certain scatter in orientation (Vony-35, Vony-44, Csek-01), but their strike tends to be around NW–SE strike (Fig. 19). Sedimentary breccia of the Rezi Dolomite is exposed in the Csókakő quarry, which is interpreted as fault-bounded talus breccia of a major basin-bounding normal fault (Cserszegtomaj Fault) by Csillag et al. (1995) and Héja et al. (2018). Based on this analogy, we interpret the Kőmell Cliff as a similar Late Triassic sedimentary breccia related to Late Triassic normal faulting. Blocks of this sedimentary breccia are frequently made up of redeposited carbonates of shallow water origin. These shallow water carbonates lithified shortly after sedimentation (Haas et al., 2021), which made its re-deposition as sedimentary breccia possible.

Fault-induced mass movements created slump folds in the Rezi Dolomite, which most probably only lithified during burial; therefore, the semi-consolidated carbonate mud was able to suffer continuous deformation. It is not always easy to distinguish slump folds and tectonic folds. The main differences in their deformation style are the following: slump folds show continuous (ductile) deformation, whereas tectonic folds developed in brittle regime in the study area. Accordingly, slump folds are often more rounded (Fig. 6c), and the thickness of the layers is frequently not uniform. In contrast, the limbs of the tectonic folds are frequently fractured or even brecciated. Slump folds can be used for estimating the direction of gravity movement; however, these reconstructions have many uncertainties. At the early stage of soft-sediment deformation, slumps are symmetric, open folds; in this stage the transport direction can be considered perpendicular to the fold axis (Bradley and Hanson, 1998). During the progressive development of slump folds, the folds become more asymmetric and arcuate. Sheath fold geometry can occur at the final stage of slump fold evolution. In that case the transport direction is parallel to the fold axis (Alsop and Marco, 2011). The Sm1 fold in the Molnárkő quarry possibly represents such a strongly asymmetric fold. On the other hand, most of the observed slump folds of the study area show slightly asymmetric geometry; therefore, we suppose hinge-perpendicular transport directions based on them (Fig. 19). Similar to the neptunian dykes, the orientations of slump fold axes show big dispersion, so they can reflect variable slope directions, or the transition from cylindrical to conical geometry. On the other hand, more than half of the measured hinges are in good agreement with extension direction deduced from syn-sedimentary faults and dykes, all indicating slope directions to NE or SW (Vony-03, 04, 21, 11-15, Csen-10).

We found several NW–SE-striking conjugate normal fault pairs, which were possibly formed before the tilting of the strata (Vony-1, Vony-11-15, Vony-35). The map-view distribution of these D2 structures is shown on Fig. 19. The pre-tilt normal faults (D2) show uniform NE–SW extensional directions, in contrast the extensional directions of the D1 structures (syn-sedimentary normal faults, slumps, neptunian dykes). This may imply that the stress field was more isotropic than during the D1 phase.

Map-scale structures of the D1 and D2 phases. Intraplatform basins formed in the southwestern part of the Transdanubian Range (KH) during the Late Triassic (Haas, 2002; Haas et al., 2012). Syn-sedimentary normal faults were always postulated along the basin margins based on sudden lithological changes or fracture-controlled dolomitization (Haas et al., 2012; Hips et al., 2015). However, direct observations and detailed description of the faults and Triassic fault-related sediments are sporadic (Budai et al., 1999a; Csillag et al., 1995). Héja et al. (2018) described the half-graben geometry of the Late Triassic basins of the KH.

The main basin-bounding Late Triassic fault of the KH is the Cserszegtomaj Fault, which is outlined based on distribution of the sedimentary breccia facies of the Rezi Dolomite (Héja et al., 2018). The NW–SE strike of this fault is in accordance with most of the mesoscale structural data (Fig. 19), which show NE–SW syn-sedimentary extension for the Late Triassic (Suppl. I.). The Cserszegtomaj Fault is strongly segmented, the overlapping segments are most probably connected by relay ramps. The scatter in orientation of slump folds and other pre-orogenic outcrop-scale extensional structures reflect the complex geometry of this strongly segmented basin-bounding fault (Fig. 19). The fracture set sub-perpendicular to the major bounding fault (Cserszegtomaj Fault) is not surprising, and typical in rifts, where transfer faults, breached relay ramps sub-perpendicular to rift segments, are abundant. This could be the case for the TR in the Jurassic (Fodor, 2008), and for the South Alpine platform (Winterer et al., 1991).

The Carnian formations of the eastern KH are bounded by major map-scale faults. These are the WNW–ESE-striking Nemesvita Fault in the north, the NW–SE-striking Ederics Fault in the south, and the N–S-striking Szt. Miklós Fault (Fig. 20). The vertical separation of these faults is significant, in some places the entire Hauptdolomit is omitted. Dudko (1996) and Budai et al. (1999a) considered the Szt. Miklós Fault to be a Cretaceous sinistral strike-slip fault. In contrast Héja et al. (2018) considered the Szt. Miklós Fault as a pre-orogenic fault, since NW–SE-striking Cretaceous tear faults (see the next sub-section for detailed description), laterally offset this structure. The (W)NW-(E)SE strike of the Ederics and the Nemesvita faults matches with the orientation of mesoscale extensional structures of the D1 and D2 phases (Fig. 19); on the other hand, the Szt. Miklós Fault should have been an oblique-slip sinistral normal fault, if it is a pre-orogenic (D1 or D2) structure.

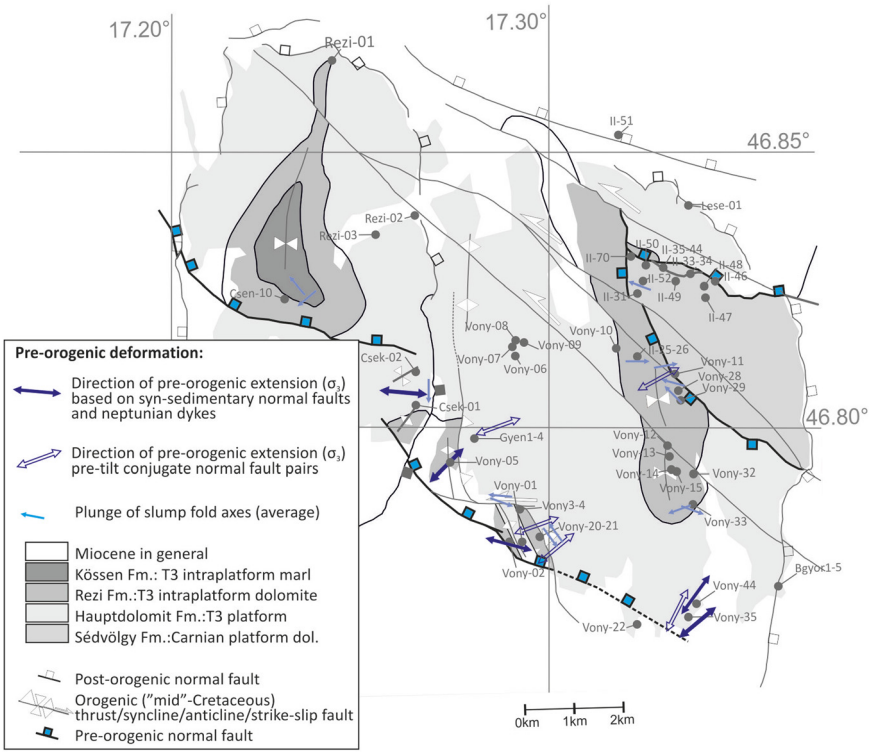

Fig. 19. Direction of extension inferred from outcrop-scale Late Triassic syn-sedimentary (D1) and pre-tilt (D2) extensional structures. For the stereoplots of the structures see Suppl. I. The trace of major map-scale pre-orogenic normal faults are based on Héja et al. (2018)

Cretaceous – Early Miocene (?) contractional deformations – D3-D5 phases

Mesoscale structures of the D3-D5 phases. A huge amount of structural data indicates the presence of compressional or transpressional deformations in the KH (Suppl. I.). It is evident in many places that tilting of the Triassic beds is the result of folding: nice outcrop-scale anticlines and synclines are exposed in the Pajtika (Fig. 4), Molnárkő (Fig. 5), Pilikán (Fig. 7) and Gyenesdiás quarries (Fig. 8). Merged dip data of scattered outcrops outline map-scale folds (e.g., Büdös-kút road cuts – Fig. 15h). Most of the fold axes range between NNE–SSW and NNW–SSE trends (Fig. 21); these structures support the presence of ~E–W shortening (Suppl. I: D3b). However, NE–SW and NW–SE-trending folds also occur (Molnárkő (Csek-01), Pajtika (Csek-02) quarries and Felsőhegy quarry (Vony-35, -44), respectively) (Fig. 21).

The dolomite is frequently fractured or even friable/powdered near the contact of the dolomite beds (e.g., Gyenesdiás eastern quarry, Balatongyörök quarry). Dolomite powdering is an enigmatic phenomenon, which has been associated with many processes including tectonism, weathering, hydrothermal fluid flow and freeze-thaw cycles in a periglacial environment (Poros et al., 2013 and references therein). We found dip-slip striae on bedding surfaces only in the Pajtika quarry. In other cases, we could not observe any sign of shearing along the powdered beds. Even so, we speculate that these friable dolomite zones are layer-parallel shear-zones associated to flexural-slip folding.

Pre-tilt thrust and strike-slip faults (D3a) show a relatively coherent pattern; based on these structures WSW–ENE to WNW–ESE compression can be supposed at the early stage of folding (Fig. 21, Suppl. I: D3a).

In contrast, the contraction directions of the post-tilt faults-slip data show diverse pattern (Fig. 22). In most cases the direction of shortening ranges from ENE–WSW to WNW–ESE regarding the post-tilt fault-slip data, similarly to the pre-tilt D3a phase: we classify these post-tilt structures to the D3c phase (Suppl. I). It should be noted that two separate phases, with slightly different directions, cannot be completely ruled out.

We classified the post-tilt structures characterized by NW–SE compressional stress field into the D4 phase (sites Csek-1, Vony-01, 6-10, Bgyö-01-05, II-47-51). This phase is represented only in 6 sites (Suppl. I.); the number of fractures is small, sometimes only 1-2, so the importance of this shortening remains modest in any scenario.

The presence of NE–SW compression deduced from striated faults is without doubt (Fig. 22, Suppl. I). In fact, thrust and strike-slip faults indicate this shortening (or compression) in quite a number of sites, and we classify these structures to the D5 phase. More importantly, the tilt test of data indicates that the NE–SW compression followed the main tilting or folding (Suppl. I).

Map-scale structures of the D3-D5 phases. In accordance with the mesoscale data, the main mapped structures in the KH are N–S trending folds (Budai et al., 1999b). Rezi Dolomite and Kössen Marl are preserved in the core of the

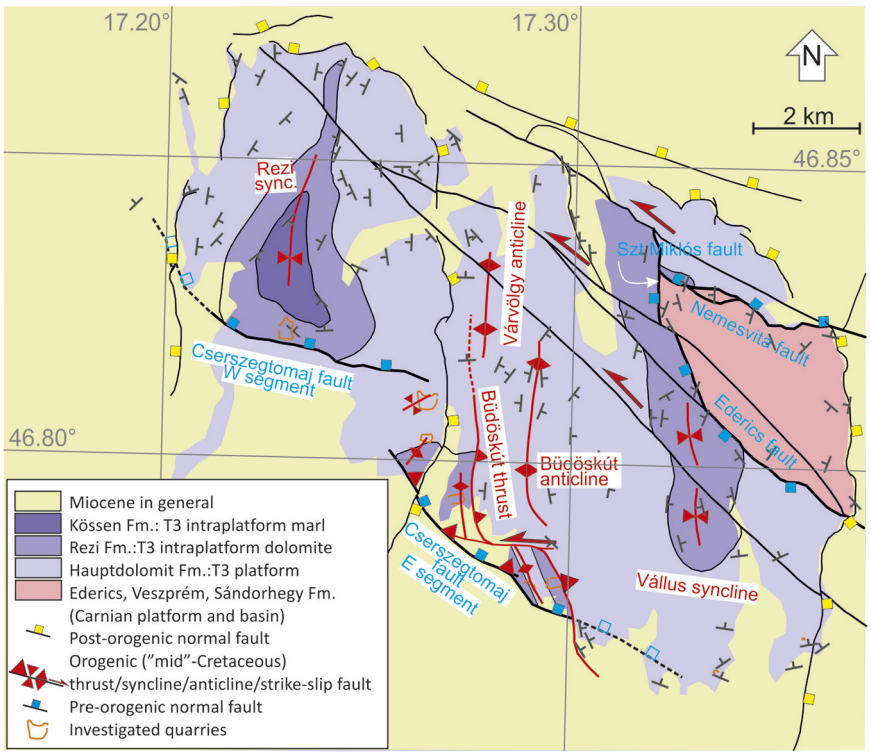

Fig. 20. Pre-Quaternary geologic map of the Keszthely Hills indicating the most important map-view pre-orogenic, orogenic and post-orogenic structures, modified after Héja et al. (2018)

Rezi syncline whereas the Vállus syncline is outlined based on the Rezi Dolomite (Fig. 20). The Rezi and Vállus synclines are separated by the broad Várvölgy anticline (Fig. 20). On the eastern limb of the Várvölgy anticline we identified a second-order anticline based on dip data, which is referred to as the Büdöskút anticline in the present study (Fig. 20). We presume that this anticline formed the hanging wall of the west-vergent Büdöskút thrust. This thrust can only be detected along the southern portion of the Büdöskút anticline, where the Hauptdolomit is thrust over the Rezi Dolomite (Fig. 20). Both the Büdöskút thrust and the associated anticline are N–S-trending; however, they become gradually NW–SE-trending southward.

The Vállus synclines are cross-cut by four NW–SE-striking faults with sinistral offset (Fig. 20). The southern three strike-slip faults merge into one segment, which dissects the Rezi syncline moderately. In our opinion, the westward-decreasing sinistral separation of these faults accommodates different amounts of E–W shortening in the two sides of this fault-zone; therefore, these structures can be considered as tear-faults which developed simultaneously with N–S-trending folds (Fig. 20). The Fpaj3 fault of the Pajtika quarry (Fig. 4a) and Fm3-5 fault-set of the Molnárkő quarry (Fig. 5a and c) provide outcrop-scale analogies for these structures. The Fm3-5 faults have similar a NW–SE strike, and left-lateral kinematics, just like map-view tear-faults of the KH. The Fm3-5 fault-set possibly accommodates different amounts of shortening on the two sides of the fault-zone, since in the northeastern side (Fig. 5c) of the Fm3-5 faults the Molnárkő anticline is much tighter than on the southwestern side (Fig. 5a). The measured oblique slickenlines on Fm3 are also characteristic for tear-faults (Ortner et al., 2015).

The age and number of folding phases – comparison with other parts of the Transdanubian Range. The main compressional structures of the TR are NE–SW-trending synclines and southeast-vergent thrusts in its central part (Bakony, Balaton Highland; Fig. 1b) (Császár et al., 1978; Császár, 1986; Fülöp and Dank, 1987; Balla and Dudko, 1989; Tari, 1994; Budai et al., 1999a, b; Albert, 2000; Kiss, 2009; Fodor, 2010; Csicsek and Fodor, 2016). In the KH and Zala Basin, the trend is N–S or even NNW–SSE (Tari, 1994; Dudko, 1996; Budai et al., 1999a; Fodor et al., 2013a). These variable trends are traditionally explained by two phases of folding with sub-perpendicular shortening directions (Tari, 1994; Tari and Horváth, 2010).

The Gerecse Hills (NE TR) represent an additional complexity, where even three different sets of folds and characteristic shortening directions seem to be present (Bada et al., 1996; Sasvári, 2008, 2009; Fodor et al., 2018), namely folds or thrust with E–W, NE–SW and NW–SE strikes. Recently Fodor et al. (2018) and Szives et al. (2018) arranged the folding in a successive deformation story, and gave time constraints for two of them.

These works, and all earlier ones (Csontos et al., 2005; Pocsai and Csontos, 2006; Sasvári, 2008, 2009) followed the concept of Tari (1994) that the (E)NE–(W)SW shortening in

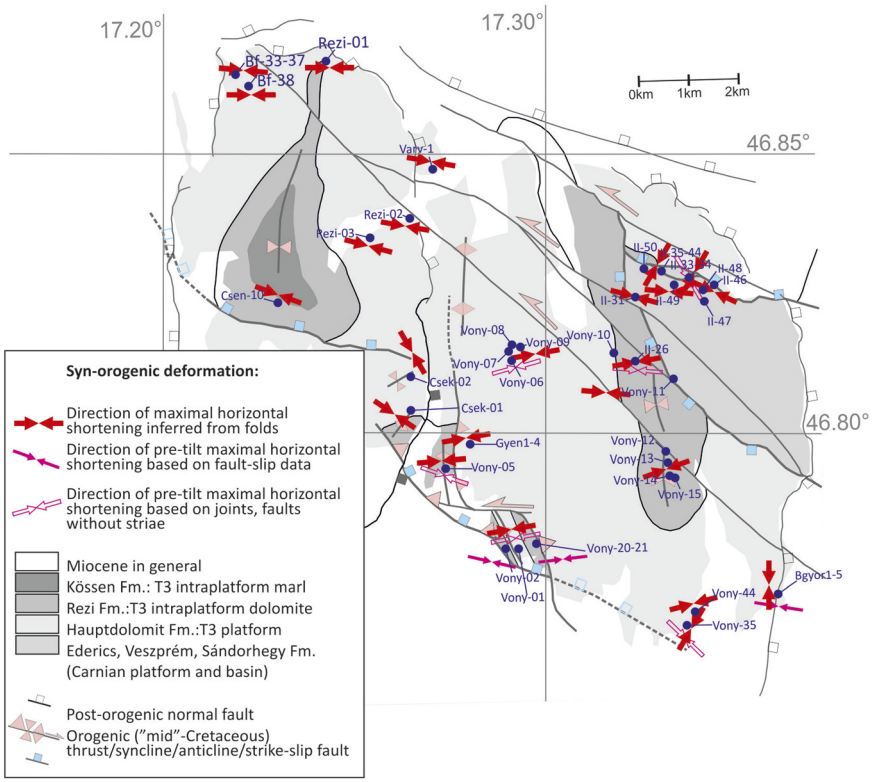

Fig. 21. Direction of maximal horizontal shortening inferred from pre-tilt (D3a) and syn-tilt (D3b) structural data. For the stereoplots of the structures see Suppl. I

the TR is related to the formation and destruction of an early Cretaceous foreland basin located only in the northeastern TR (Fig. 1b). Since the source of detrital sediments is clearly the obducted Neotethyan oceanic lithosphere, its obduction and mainly the post-obduction deformation onto the Adriatic margin is the source of folding, due to NE–SW shortening.

The main question is how far this folding could be projected southwestward, into the central and the southwestern TR. Tari (1994) adopted this scenario and explained the variable thrust directions by a two-fold deformation history, with an early Aptian top-to-SW thrusting later overprinted by an Albian (N)NW-(S)SE contraction, which can be correlated with the formation of the Austroalpine nappes. Pocsai and Csontos (2006) suggested an Aptian initiation of NE–SW shortening in the central TR.

The huge stratigraphic gap between the folded Upper Triassic and the Miocene cover makes the timing of the D3-5 phases of the study area difficult. Therefore, we correlated the deformation phases of the KH and the other parts of the TR, based on previous works (Fig. 23).

Following the concept of Tari (1994), **the first scenario** can be that the E–W shortening of the KH is the equivalent of the Aptian "obduction–related" deformation of the TR (Fig. 23). Tari (1994) and Tari and Horváth (2010) considered the W-directed thrusts of the Zala Basin as a result of this phase. This is supported by pre-tilt fault-slip data, which suggest that the early phase of shortening can be characterized by an E–W direction (Suppl. I., Fig. 23). Following this line of thought, the few data indicating NW–SE compression (D4) would correspond to the Albian "Austroalpine" deformation of Tari (1994).

On the other hand, near Sümeg (between the KH and the Bakony Mts.) strongly tilted Aptian – Lowermost Albian Tata Limestone occur in the core of the NNE–SSW-trending syncline (Fig. 1b, Haas et al., 1984), The observed shortening direction (~WNW–ESE; Fodor, 2010) is an intermediate direction between NW–SW (Bakony Mts., Balaton Highland) and E–W (KH). While the transition is spatially gradual, we may consider all these contractional structures as having been related to the main phase of folding induced by NW–SE shortening (**second scenario,** Fig. 23). The Sümeg example constraints the WNW–ESE shortening as post-Aptian. The connection of folds between the two areas separated by the Miocene Tapolca Graben is expressed by the gradual change, and spatial variations, of E–W to NW–SE shortening directions (Fig. 1b). We can exclude that our D5 phase (Suppl. I.) corresponds to the Aptian NE–SW compression of Tari (1994), since all the related fault-slip data postdates tilting. This enigmatic phase was sporadically measured on Upper Cretaceous rocks by Kiss (2009) and Fodor (2010), which can represent the analogue of the observations in the KH; this would place this phase into the latest Cretaceous to Paleocene interval (**second scenario,** Fig. 23).

It should be noted, however, that latest Cretaceous to Paleogene deformations cannot be responsible for the formations of the NW–SE-trending folds in the KH (e.g., Felső-

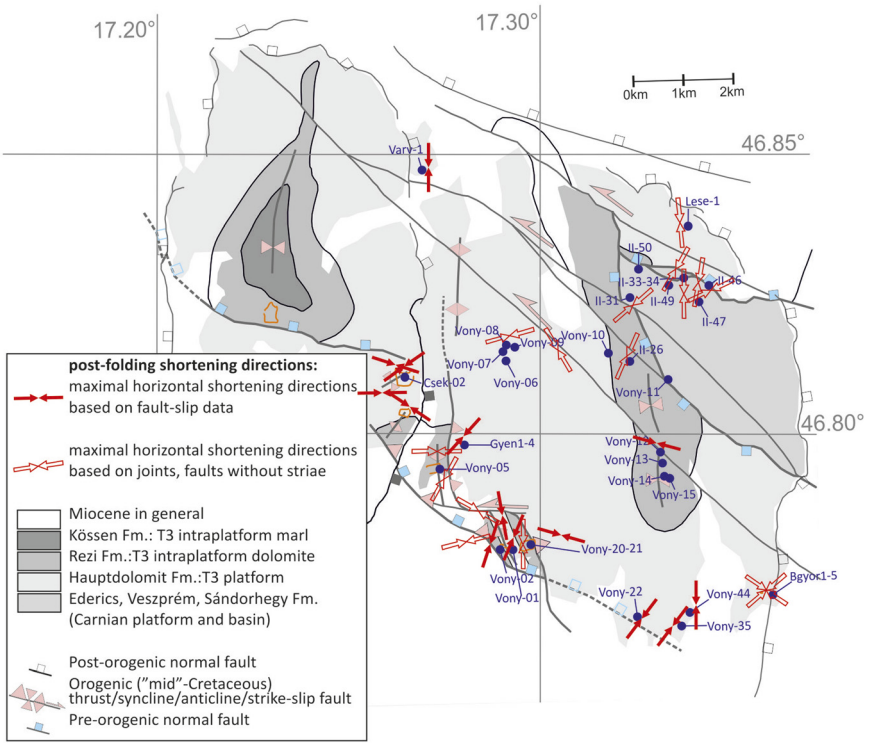

Fig. 22. Direction of maximal horizontal shortening inferred from post-tilt structural data (D3c, D4 and D5 phases). For the stereoplots of the structures see Suppl. I

hegy quarry; Fig. 20), since the sub-horizontal Upper Cretaceous beds in the northern and western surroundings of the KH (Haas et al., 1984; Fodor et al., 2013a) excludes the possibility of significant post-Senonian folding. Thus, to explain the presence of folds with NE–SW shortening and faults due to NE–SW compression one should suggest a more complex scenario, and potentially the reoccurrence of the NE–SW shortening.

In a recent paper, Héja et al. (2022) give an alternative interpretation for the three generation of folds in the KH. This concept (**third scenario**, Fig. 23) takes into account that the dominant shortening direction is E–W, and a certain variation in the shortening/compression direction is related to the oblique inversion of Late Triassic and Jurassic extensional grabens. Such a distortion of the S_{Hmax} trajectory might have resulted in folds with NW–SE axes near the main pre-orogenic faults. This model implies that the pre-existing normal faults and the breached relay ramps connecting them promote the formation of oblique and lateral ramps in the KH. It is also possible that such oblique inversion of a segmented graben system resulted in the development of a heterogeneous stress field, whose stress trajectory can show important variations (Fodor, 2019). The NW–SW shortening could have occurred on these inverted relay ramps (Héja et al., 2022). Deviation of the shortening directions along oblique and lateral ramps have been documented in many fold and thrust belts based on fault-slip data (e.g., Ustaszewsky and Schmid, 2006).

One should also take into account that stress fields with similar σ_1 may have repeatedly reappeared during the evolution of the TR (Suppl. I.). Therefore, we cannot exclude that the classification of some of the post-tilt fault-slip data could be erroneous. For example, the post-folding D3c (E–W compression) and D4 phases (NW–SE compression) could also belong to either the middle Eocene to Oligocene basin formation, or to the Late Oligocene – Early Miocene dextral slip of the Mid-Hungarian Shear-zone (Fodor et al., 1999) (**third scenario,** Fig. 23). However, this alternative interpretation does not concern the folds which should be pre-Senonian (see above).

Miocene extensional deformations

The pre-rift extension: D6 deformation phase and its stress field. The D6 stress field is marked by NE–SW extension, the minimal stress axis of which shows a slight dispersion toward ENE–WSW (Fig. 24). The main structures are NW–SE-striking normal faults; moreover, there are a few oblique dextral-normal faults striking somewhat toward WNW–ESE (Vony-02, -22, Figs 10g and 11b, Suppl. I.). These oblique slip faults are possibly reactivated normal faults, which were formed due to NNE–SSW extension.

The faults of this phase were also prone to reactivation, frequently by oblique slip, during the successive D7 phase (e.g., Fig. 5d). No direct timing is available for this stress field, but the relative chronology, the analogy from other parts of the TR (Márton and Fodor, 2003; Fodor, 2019), and the parallelism of the surface faults to graben-bounding main normal faults of the surrounding Zala and Danube basins (Tari, 1994; Csontos, 1995; Fodor et al., 2013a, 2021),

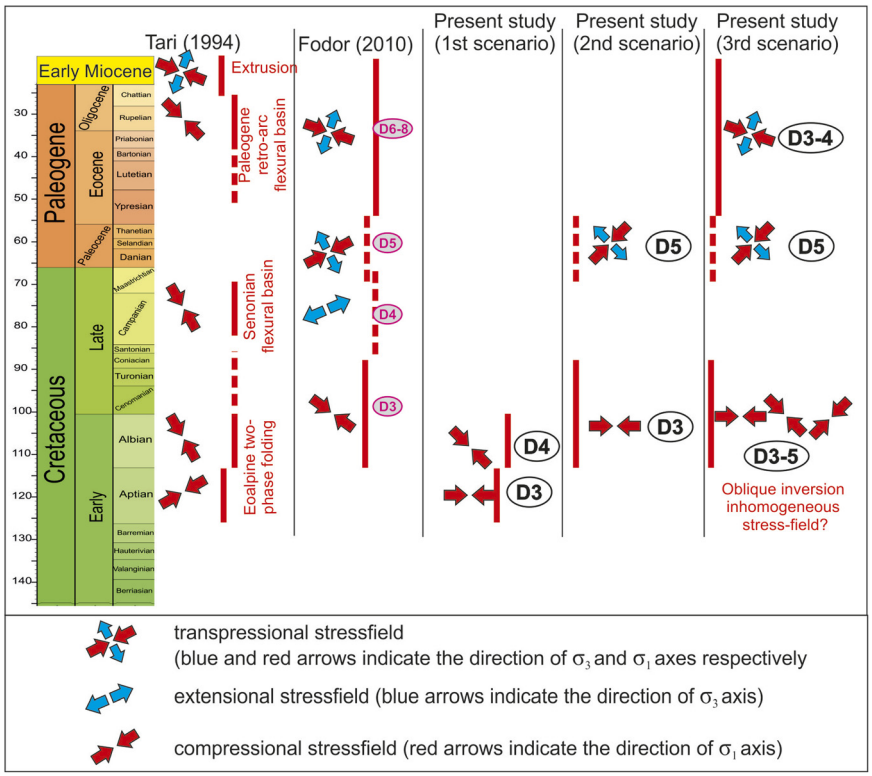

Fig. 23. Correlation of the deformation phases of the KH and the other parts of the TR. The first two columns show the temporal variations of stress fields based on Tari (1994) and Fodor (2010) respectively. The third and fourth columns (first and second scenarios) are the correlation of our results with the models of Tari (1994) and Fodor (2010), respectively. In the last column (third scenario) we considered the various trending folds of the KH as the result of one single deformation, which was a consequence of oblique inversion of pre-existing faults, causing a heterogeneous stress field (Héja et al., 2022). In this third scenario we also supposed that the compressional/transpressional stress fields with E–W (D3), NW–SE (D4) and NE–SW (D5) directed σ_1 might have been repeatedly recurrent during the Late Cretaceous and Cenozoic. These stress fields appear in the post-tilt fault slip data

suggest Miocene timing. In fact, in the neighboring Zala Basin this stress field marks the major syn-rift faulting and related subsidence (Csontos, 1995; Fodor et al., 1999, 2013a, 2021; Nyíri et al., 2021). However, in the KH no coeval sedimentation occurred. Instead, this was still the time of terrestrial denudation and karstification (Kelemen et al., 2021).

Despite the relative frequency of outcrop-scale (meso-scale) fractures, very few map-scale features belong to this deformation phase. Possibly the northeastern boundary fault of the KH could have been initiated during this phase (Figs 20 and 24), although later reactivation could obliterate the signs of this earlier D6 deformation.

The Miocene syn-rift extension: the D7 phase, D7a and D7b stress states. The next D7 phase was marked by two somewhat distinct stress fields. The merging of these two stress states into one phase is our interpretation; other solutions will also be discussed. Stress field D7a is a strike-slip, locally compressional field with the maximal stress axis close to N–S and σ_3 is either vertical or trending E–W (Fig. 22, Suppl. I.). In addition to E–W-trending reverse faults and low-angle fractures (potentially also shear fractures with reverse sense), conjugate strike-slip faults; dextral in NW–SE and sinistral in NE–SW orientation, are also present (Suppl. I., Figs 10f, 12b, 15c and 16c). In addition to the post-tilt character of this stress field, in the sites Vony-02 and Varv-01 there is one relative chronology criterion. A few NW–SE-trending dextral faults have a dip of ~60°, and seem to have reactivated fracture planes, which were most probably formed during the previous D6 NE–SW extension (Fig. 10). If this relationship can be extrapolated, then the N–S compression would be younger than the NE–SW extension (D6), although a different succession is also possible.

The dextral faults, particularly those with small normal component, could have played a role in the formation (or reactivation) of the northeastern boundary fault of the KH, or in the Nagygörbő and Vasvár grabens more to the NW. The dextral slip on the NW-trending faults can be combined with normal slip of the N–S faults of the KH and the surrounding grabens. This is the reason why we consider that strike-slip faults with N–S compression can be spatially connected to E–W extension.

In a second alternative solution, the D7a strike-slip faulting would be the very typical deformation of the TR. This is composed of the classical WNW–ESE-trending dextral faults, described by many authors (Kókay, 1976; Mészáros, 1982, 1983; Tari, 1991; Kiss and Fodor, 2007;

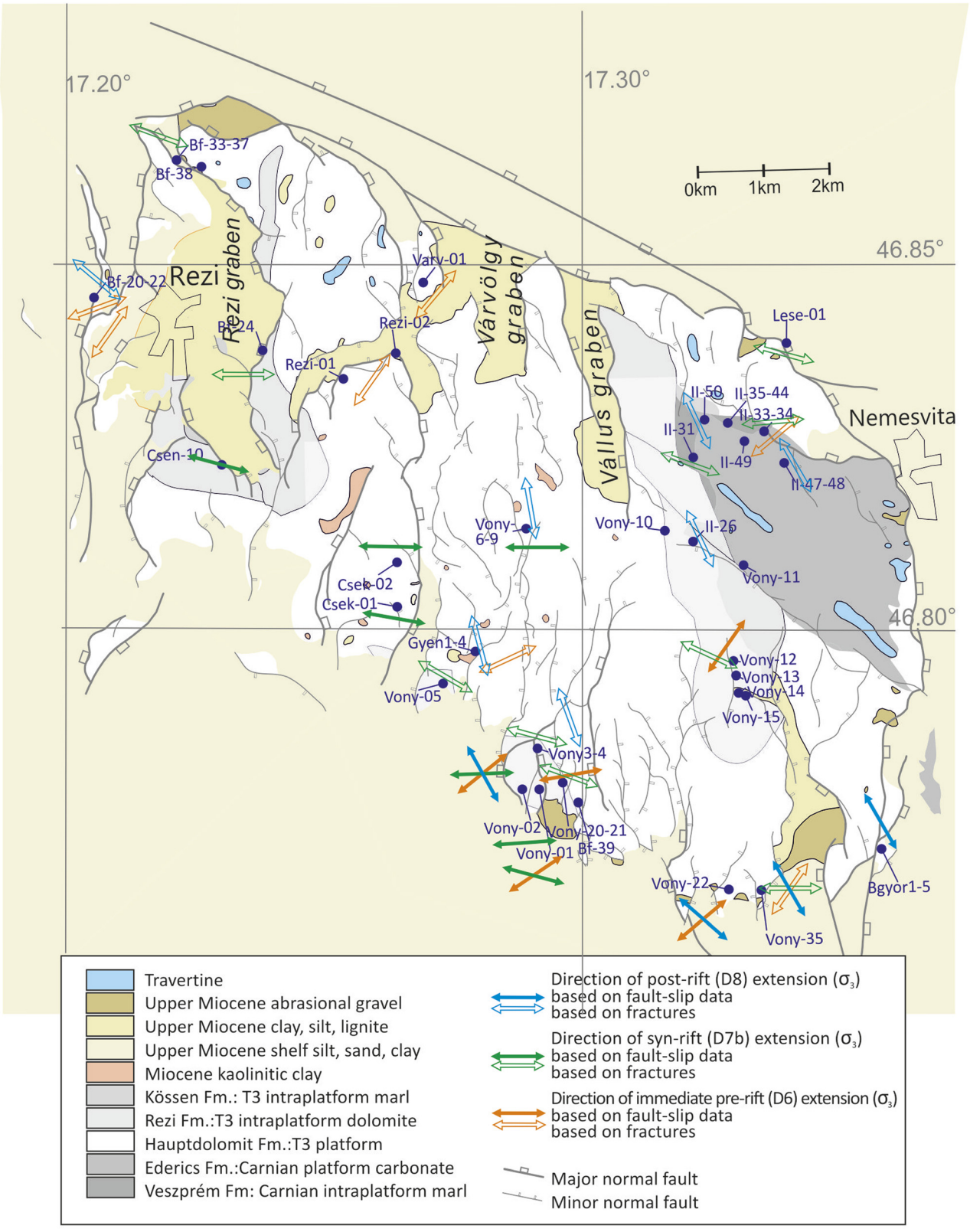

Fig. 24. Direction of extension inferred from post-tilt (D6, D7b, D8) extensional structures. For the stereoplots of the structures see Suppl. I

Sasvári et al., 2007), and obviously marked in the morphology (Zámolyi et al., 2010). The timing of this transpression is middle Miocene, and locally can be constrained to the Sarmatian (Kókay, 1956, 1976, 1996). This transpressional deformation extends till the Balaton Fault in the east, where a more or less continuous Late Badenian to Early Pannonian sinistral transpression has been demonstrated (Balla et al., 1987; Várkonyi et al., 2013; Visnovitz et al., 2015). The sinistral Balaton Fault would be the conjugate of the intra-TR dextral faults, as suggested in his elegant model by Tari (1991). It is not yet clear how and when extensional deformation, also Middle Miocene in age, were combined with this transpression. This could be spatial or temporal changes, or a strongly heterogeneous, transpressional to extensional strain field. It is also possible that the magnitudes of the σ_1 and σ_2 stresses were close to each other, causing stress axis permutation.

D7b represents an extensional deformation where the minimal stress axis was oriented E–W. The direction of σ_3 axes varied from E–W to ESE–WNW. The main conjugate normal faults, a few deformation bands and numerous joints trend N–S (typical examples are II-31, Vony-01, -02, -03, Suppl. I). Locally, dextral-normal oblique-slip faults (Suppl. 1, sites Csek-01, Vony-02) and pure dextral faults were also associated with the extension (sites Csek-02, Vony-11-15). In some Miocene sites, the direction of fractures shows variations; in these cases, some of the sub-vertical faults are considered as strike-slip faults (Fig. 18., sites Bf-33-37, Bf-18). Examples of this stress field were presented by Héja (2015) and by Fodor et al. (2017, 2021) in the KH; our present data base summarizes all of our previously published and unpublished measurements (Suppl. I.). It should be noted that Dudko in Budai et al. (1999a) presented a similar fracture pattern measured in Upper Miocene rocks, although these data were not interpreted in terms of stress. In addition, Sztanó et al. (2010) found N–S-trending normal faults in the Billege gravel pit in the Tapolca Graben: these structures also belong to this phase. This stress field is widely documented throughout the entire Pannonian Basin (Fodor et al., 1999; Fodor, 2010, 2019) and was considered as one important phase of the rifting process (Csontos et al., 1991; Fodor et al., 1999; Sasvári et al., 2007; Bodor, 2011; Sipos-Benkő et al., 2014; Petrik et al., 2016) and corresponds to the regional D10 phase of Fodor (2008, 2010). We adopted the classification of Fodor et al. (2021), that this extension locally represents the main syn-rift phase of this part of the PB.

Some of the observations indicate that this stress field affected the Upper Miocene sediments within the KH and in the surroundings, namely the Tapolca Graben to the east. These structures include a sandstone dyke in the T3 dolomite (site Csen-10, Fig. 3a and d), a syn-sedimentary fault in the site Lese-01 (Fig. 15) and fractures, partly syn-sedimentary, in the Hosszú-völgy (Fig. 18, sites Bf-33-37, Bf-38). Deformation bands in site Bf-39 were formed at shallow burial, close to the time of sedimentation. In site Bf-38 faults were observed in large Triassic boulders of the Late Miocene abrasional conglomerate (fractured pebbles, Fig. 18).

At map scale a great number of faults can be connected to the extension. Although earlier maps or other publications indicated some of the faults (Bohn, 1979; Dudko et al., 1992; Csillag and Nádor, 1997; Budai et al., 1999a), the most detailed compilation is from the last work of Fodor et al. (2021). From it we adopted this map, which neglects Quaternary formations (Fig. 24). The faults were delineated on the basis of the distribution of Middle Miocene karst infillings, Upper Miocene sediments, the presence of steep slopes, often controlling deep valleys and bounding the Keszthely horst itself. The distribution of abrasional gravel, conglomerate or conglomeratic breccia also indicates the presence of fault scarps. The N–S-striking fault-controlled steep slopes in the morphology are considered to be eroded fault scarps.

The fault geometry is typical for extensional regions; the faults show frequent strike changes, curved traces, debranching, merging. Deviation from N–S to either NE–SW or NW–SE is a typical feature, and partly can be interpreted as true kinematic changes from normal to strike-slip character. Partially overlapping segments form relay ramps, which are generally breached by connecting splays and thus form a strongly curved continuous trace (Fig. 24).

Faulting was associated with the modest tilting of Miocene layers and the denudation surfaces. Csillag and Nádor (1997) mapped the main faults and suggested 20–100 m of throw based on the displaced pre-Pannonian denudation surfaces. Tilting was shown on morphological cross-section within the KH (Fodor et al., 2021). These cross-sections show that the eastern and northern boundary faults could accumulate 400–600 m of normal throw. Tilting also occurred in the Tapolca and Várvölgy grabens (Fig. 24) demonstrated by cross sections based on boreholes (Csillag et al., 2004, 2010). The Rezi graben (Fig. 24) is also a tilted block, bounded by the main fault in the east, while the graben north of Keszthely is east-facing. In the case of the narrow, NW–SE-striking Hosszú Valley, dextral-normal kinematics is probable (Fig. 18).

The presence of conjugate normal faults, dip-slip striae, and the calculated and estimated direction of extension argue for normal kinematics for the N–S-trending faults (Suppl. I.). On the northeastern side the NW-trending boundary fault zone of the KH (Figs 20 and 24) could have a pure dextral or oblique dextral-normal fault, as suggested by the stress field and also by mesoscale faults in sites Varv-1, Csek-1. In the SW, no such linear, continuous boundary fault is present (Fig. 24); instead, a system of parallel, probably en-echelon faults may indicate a similar dextral shear zone at depth.

Fault-controlled valleys were flooded by the Late Miocene lacustrine transgression around 10 Ma within the KH, suggesting a pre-10Ma initiation of faulting. On the other hand, at the periphery of the KH, the N–S faults were covered by abrasional gravel, conglomerate, or more angular breccias, suggesting that the KH represented a shallow fault-bounded horst during the Pannonian, after ~10 Ma. Cross sections also show that some Late Miocene units thickening toward the eastern or northern boundary faults, suggesting syn-sedimentary activity, and steep basin-bounding slope

(Csillag et al., 2010). One of the interesting morphotectonic features is the Hosszú Valley in the NW KH that we analyzed in section 4. The long and narrow valley geometry and the steep slope on both sides argue for a tectonic feature, possibly a fault-bounded oblique-slip graben filled with Upper Miocene deposits. The presence of sub-angular to rounded clasts, often with fractures infilled with Miocene sand, or striated external surfaces, suggest active faulting along the eastern fault scarp during the deposition of the fault-bounded talus apron.

All these observations demonstrate that faulting was active in the Late Miocene. Fodor et al. (2021) collected arguments that this extension started in the Late Badenian, between 15 and 14.5 Ma when the subsidence of the Tapolca and Várvölgy grabens started, and when the terrestrial karstification and doline formation terminated in the Keszthely plateau (Kelemen et al., 2021). Cross-sections in the Tapolca Graben and sedimentary studies clearly argue for early Late Miocene syn-sedimentary faulting (Csillag et al., 2010). These data led Fodor et al. (2021) to consider a time span of 14.5 to ~8 Ma for the syn-rift faulting, which belongs to phase D7b stress field.

Miocene post-rift extension: the D8 stress field. This stress field was found only in 11 sites (Suppl. I.). The main outcrop-scale features are ENE–WSW-trending normal faults and joints. Oblique-slip faults also belong to the stress field: N–S-trending dextral oblique faults in site Vony-02 and Bgyö-1-5, and E–W-trending sinistral-normal faults in site Vony-35. The deduced stress field was extensional, with σ_3 in SSE–NNW direction. No map-scale feature was unambiguously attributed to this stress field.

The timing of this stress field is problematic due to the lack of direct chronological criteria. On the other hand, the fractures are always post-tilt, and, based on the relative chronology between fractures, it is always younger than the D2–D6 phases. In site Vony-02, the D8 stress field is convincingly older than the D7, while in site Vony-06 the less conclusive single criterion would suggest opposite chronology. Thus, we interpret the D8 as an expression of weak post-rift faulting, which could have occurred after ~8Ma. Alternatively, this stress field would only represent spatial variation of the D7 stress field. Similar rotation of stress axes from E–W to (S)SE–(W)NW extension direction is present in other parts of the Pannonian Basin (Fodor et al., 1999; Bodor, 2011; Sipos-Benkő et al., 2014; Petrik, 2016; Petrik et al., 2016) and was interpreted as having been connected to regional change in shortening direction within the Carpathian orogenic belt (Csontos et al., 1991; Fodor et al., 1999; Fodor, 2010).

CONCLUSION

We applied extended field structural measurements and stress field analysis to reveal the multistage deformation history of the KH. Our detailed approach resulted in the documentation of a huge number of structural elements in quarries and outcrops within the investigated area. During our detailed analyses, our most important findings are the following ones:

1. We identified Late Triassic syn-sedimentary structures (slump-folds, faults) and pre-orogenic pre-tilt structures in 10 localities (D1, D2). The orientation of the structures shows considerable dispersion; however, most data suggest NE–SW extension.
2. Structural manifestation of late Early Cretaceous to Early Miocene (?) shortening was documented in all Mesozoic outcrops. The measured thrusts, strike-slip faults and estimated fold axes indicate multidirectional shortening in E–W, NW–SE, NE–SW directions. We discussed three different scenarios for the interpretation, starting with an interpretation of distinct, successive phases to a preferred solution of a single complex inhomogeneous stress field. We put our vote on the importance of pre-orogenic structures, which fundamentally influenced the geometry of the orogenic structures, such as orientation of fold axes and thrust planes. Thus, we interpreted all three directions of the main tilting event as the results of one stress field, with local varieties of stress states due to oblique inversion of pre-orogenic faults.
3. The post-tilt extensional deformations are related to the evolution of the Pannonian Basin. The early signs of these deformations are characterized by NNE–SSW or NE–SW extension (D6). It was followed by a poorly-dated transpressional event due to N–S compression and E–W extension (D7a). The D6 and D7a deformations were not connected to sedimentation, and have little expression in map-scale faults. On the other hand, E–W extension (D7b) locally represents the main faulting phase and resulted in the formation of N–S-striking normal faults and NW–SE-striking dextral-normal faults. This deformation could start after a long-lasting karstification at ca. 14.5 Ma, and was still active during the flooding of the Lake Pannon after ~10 Ma. A poorly represented ESE–NNW extension (D8) could be connected to a weak post-rift fracturing of the area.

ACKNOWLEDGEMENT

The research was supported by the National Research Fund of Hungary (NKFI) OTKA, grants 113013, 134873. Discussions with Tamás Budai and János Haas are greatly acknowledged. We benefitted from the field discussion of Orsolya Sztanó and Krisztina Sebe concerning the Late Miocene sedimentation and related deformation. We are grateful for the help of Róbert Arató, János Csizmeg, Vencel Lavrotyi, Anita Nyerges and Balázs Soós, who took part in the collection of structural data. The technical help of Barbara Beke is also acknowledged. The comments of the two reviewers (Attila Petrik and Gyula Maros) and the editor (Norbert Németh) highly improved the clarity of the manuscript.

SUPPLEMENTARY MATERIAL

Supplementary data to this article can be found online at https://doi.org/10.1556/24.2022.00114.

REFERENCES

Albert, G. (2000). *Az Északi-Bakony gyűrődései. (in Hungarian)*. MSc thesis, manuscript, Eötvös University, Dept. of General and Applied Geology, p. 89.

Alsop, G.I. and Marco, S. (2011). Soft-sediment deformation within seismogenic slumps of the dead sea basin. *Journal of Structural Geology*, 33(4): 433–457, http://doi.org/10.1016/j.jsg.2011.02.003.

Anderson, E.M. (1951). *The dynamics of faulting and dyke formation with application to Britain*, 2nd ed. Oliver & Boyd, Edinborough, p. 206.

Angelier, J. (1984). Tectonic analysis of fault slip data sets. *Journal of Geophysical Research*, 89(B7): 5835–5848, https://doi.org/10.1029/jb089ib07p05835.

Angelier, J. (1990). Inversion of field data in fault tectonics to obtain the regional stress – III. A new rapid direct inversion method by analytical means. *Geophysical Journal International*, 103: 363–373.

Angelier, J. and Manoussis, S. (1980). Classification automatique et distinction des phases superposée en tectonique de failles. In: *Comptes Rendus de l'Académie des Sciences, Paris 290, série D*, pp. 651–654.

Bada, G., Fodor L., Székely B., and Timár G. (1996). Tertiary brittle faulting and stress field ecolution in the Gerecse Mountains, northern Hungary. *Tectonophysics*, 255, pp. 269–289.

Balázs, A., Maţenco, L., Magyar, I., Horváth, F., and Cloetingh, S. (2016). The link between tectonics and sedimentation in back-arc basins: new genetic constraints from the analysis of the Pannonian Basin. *Tectonics*, 35: 1526–1559, http://doi.org/10.1002/2015TC004109.

Balázs, A., Burov, E., Maţenco, L., Vogt, K., Francois, T., and Cloetingh, S. (2017). Symmetry during the syn- and post-rift evolution of extensional back-arc basins: the role of inherited orogenic structures. *Earth and Planetary Science Letters*, 462: 86–98, https://doi.org/10.1016/j.epsl.2017.01.015.

Balla, Z. and Dudko, A. (1989). Large-scale tertiary strike-slip displacements recorded in the structure of the transdanubian range. *Geophysical Transactions*, 35(1–2): 3–63.

Balla, Z., Dudko, A., and Redler-Tátrai, M. (1987). *A Közép-Dunántúl fiatal tektonikája földtani és geofizikai adatok alapján (Young tectonics of Mid-Transdanubia based on geological and geophysical data, in Hungarian with English abstract)*. Annual Report of the Eötvös Lóránd Geophysical Institute for 1986, pp. 74–94.

Bárdossy, G. (1959). Adatok a cserszegtomaji kaolinos agyag ismeretéhez (in Hungarian). *Földtani Közlöny*, 89(4): 374–380.

Bence, G., Peregi, Z., Miszlivecz, E., and Turczi, G. (1982). *Zalaszántó. Észlelési földtani térkép. A Balaton-felvidék földtani térképe 1:20 000-es sorozat*. Data Repository of the Mining and Geological Survey of Hungary.

Benkó, Zs., Molnár, F., Lespinasse, M., and Váczi, T. (2014). Evidence for exhumation of a granite intrusion in a regional extensional stress regime based on coupled microstructural and fluid inclusion plane studies: an example from the Velence Mts., Hungary. *Journal of Structural Geology*, 65: 44–58.

Bodor, B. (2011). *A Hernád-árok szerkezetföldtani vizsgálata (in Hungarian)*. MSc thesis, Eötvös University, Department of Regional Geology, p. 99.

Bohn, P. (1979). A Keszthelyi-hegység regionális földtana (The regional geology of the Keszthely Mountains). *Geologica Hungarica. Series Geologica*, 19: 191.

Bradley, D. and Hanson, L. (1998). Paleoslope analysis of slump folds in the Devonian Flysch of Maine. *The Journal of Geology*, 106(3): 305–318, http://doi.org/10.1086/516024.

Budai, T. and Koloszár, L. (1987). A Keszthelyi-hegység nóri–raeti képződményeinek rétegtani vizsgálata. *Földtani Közlöny*, 117: 121–130.

Budai, T. and Kovács, S. (1986). A Rezi Dolomit rétegtani helyzete a Keszthelyi-hegységben. In: *Magyar Állami Földtani Intézet Évi Jelentése 1984. évről*, pp. 175–191.

Budai, T. and Muntyán, Cs. (1983). *Várvölgy. Észlelési térkép. A Balaton-felvidék földtani térképe 1:20 000-es sorozat*. Data Repository of the Mining and Geological Survey of Hungary.

Budai, T. and Vörös, A. (1992). Middle Triassic history of the Balaton Highland: extensional tectonics and basin evolution. *Acta Geologica Hungarica*, 35(3): 237–250.

Budai, T. and Vörös, A. (1993). The Middle Triassic events of the Transdanubian Central Range in the frame of the Alpine evolution. *Acta Geologica Hungarica*, 36(1): 3–13.

Budai, T. and Vörös, A. (2006). Middle Triassic platform and basin evolution of the Southern Bakony Mountains (Transdanubian Range, Hungary). *Rivista Italiana di Paleontologia e stratigrafia*, 112(3): 359–371.

Budai, T., Császár, G., Csillag, G., Dudko, A., Koloszár, L., and Majoros, Gy. (1999a). *Geology of the Balaton Highland. Explanation to the geological map of the Balaton Highland (1:50 000)*. Geological Institute of Hungary, Budapest, pp. 169–257.

Budai, T., Csillag, G., Dudko, A., and Koloszár, L. (1999b). *Geological map of Balaton Highland (1:50 000)*. Geological Institute of Hungary, Budapest.

Budai, T., Csillag, G., Vörös, A., and Dosztály, L. (2001). Középső– és késő–triász platform- és medencefáciesek a Veszprémi-fennsíkon (Middle to Late Triassic platform and basin facies of the Veszprém Plateau, Transdanubian Range, Hungary, in Hungarian with English abstract). *Földtani Közlöny*, 131(1–2): 37–70.

Császár, G. (1986). Dunántúli-középhegységi középső-kréta képződmények rétegtana és kapcsolata a bauxitképződéssel. *Geologica Hungarica Series*, 23: 295.

Császár, G., Haas, J., and Jocháné-Edelényi, E. (1978). *A Dunántúli-középhegység bauxitföldtani térképe, 1:100 000*. Geological Institute of Hungary, Budapest.

Csicsek, Á.L. and Fodor, L. (2016). Középső-triász képződmények pikkelyeződése a bakonyi Öskü környékén (Imbrication of Middle Triassic rocks near Öskü, Bakony Hills, Western Hungary, in Hungarian with English abstract). *Földtani Közlöny*, 146(4): 355–370.

Csillag, G. and Nádor, A. (1997). Multi-phase geomorphological evolution of the Keszthely Mountains (SW-Transdanubia) and

karstic recharge of the Hévíz lake. *Zeitschrift für Geomorphologie*, 110: 15–26.

Csillag, G., Budai, T., Gyalog, L., and Koloszár, L. (1995). Contribution to the upper Triassic geology of the Keszthely Mountains (Transdanubian Range), western Hungary. *Acta Geologica Hungarica*, 38(2): 111–129.

Csillag, G., Fodor, L., Müller, P., and Benkő, K. (2004). Denudation surfaces, development of Pannonian formations and facies distribution indicate Late Miocene to Quaternary deformation of the Transdanubian Range. *Geolines*, 17: 26–27.

Csillag, G., Gyalog, L., and Kovács, T. (1983). *Keszthely-K. Észlelési térkép. A Balaton-felvidék földtani térképe 1:20 000-es sorozat*. Data Repository of the Mining and Geological Survey of Hungary.

Csillag, G., Sztanó, O., Magyar, I., and Hámori, Z. (2010). A Kállai Kavics települési helyzete a Tapolcai-medencében geoelektromos szelvények és fúrási adatok tükrében. *Földtani Közlöny*, 140(2): 183–196.

Csillag, P.-né. (1959). A cserszegtomaji tűzállóagyag és festékföld. In: *Magyar Állami Földtani Intézet Évi Jelentése 1955–56. évről*, pp. 29–36.

Csontos, L. (1995). Cenozoic tectonic evolution of the Intra-Carpathian area: a review. *Acta Vulcanologica*, 7: 1–13.

Csontos, L. and Vörös, A. (2004). Mesozoic plate tectonic reconstruction of the Carpathian region. *Palaeogeography, Paleoclimatology, Palaeoecology*, 210: 1–56.

Csontos, L., Tari, G., Bergerat, F., and Fodor, L. (1991). Evolution of the stress fields in the Carpatho-Pannonian area during the Neogene. *Tectonophysics*, 199: 73–91.

Csontos, L., Sztanó, O., Pocsai, T., Bárány, M., Palotai, M., and Wettstein, E. (2005). Late jurassic-early cretaceous alpine deformation events in the light of redeposited sediments. *Geolines*, 19: 29–31.

Dudko, A (1996). *A Balaton-felvidék szerkezete (fedetlen földtani térkép alapján)*. Manuscript, Geological Institute of Hungary, Budapest.

Dudko, A., Bence, G., and Selmeczi, I. (1992). Miocén medencék kialakulása a Dunántúli-Középhegység DNy-i részén. In: *Magyar Állami Földtani Intézet Évi Jelenetése 1990*, pp. 107–124.

Erdélyi Fazekas, J. (1943). A Balaton-felvidék geológiai és hegyszerkezeti viszonyai a Veszprémi fennsíkon és Vilonya környékén. *Földt. Int. Évk*, 36(3): 3–29.

Fodor, L. (2010). *Mezozoos-kainozoos feszültségmezők és törésrendszerek a Pannon-medence ÉNy-i részén – módszertan és szerkezeti elemzés*. Doctoral thesis of the Hungarian Academy of Sciences, manuscript, p. 129.

Fodor, L. (2019). Results, problems and future tasks of palaeostress and fault-slip analyses in the Pannonian Basin: the Hungarian contribution. *Földtani Közlöny*, 149(4): 297–326.

Fodor, L. (2008). Structural geology. In: Budai, T. and Fodor, L. (Eds.), *Geology of the Vértes Hills. Explanatory book to the geological map of the Vértes Hills 1:50000*, Vol. 145–202. Magyar Állami Földtani Intézet, pp. 282–300.

Fodor, L., Magyari, Á., Fogarasi, A., and Palotás, K. (1994). Tercier szerkezetfejlődés és késő paleogén üledékképződés a Budai-hegységben. A Budai-vonal új értelmezése (Tertiarx tectonics and Late Paleogene sedimentation in the Buda Hills, Hungary. A new interpretation of the Buda Line. Hungarian with English abstract). *Földtani Közlöny*, 124(2): 129–305.

Fodor, L., Csontos, L., Bada, G., Györfi, I., and Benkovics, L. (1999). Tertiary tectonic evolution of the Pannonian Basin System and neighbouring orogens: a new synthesis of palaeostress data. *Geological Society, London, Special Publications*, 156: 295–334.

Fodor, L., Uhrin, A., Palotás, K., Selmeczi, I., Tóthné Makk, Á, Rižnar, I., Trajanova, M., Rifelj, H., Jelen, B., Budai, T., Koroknai, B., Mozetič, S., Nádor, A., and Lapanje, A. (2013a). Geological and structural model of the Mura–Zala Basin and its rims as a basis for hydrogeological analysis (in Hungarian with English abstract). *Magyar Állami Földtani Intézet Évi Jelentése*, 2011: 47–92.

Fodor, L., Sztanó, O., and Kövér, Sz. (2013b). Mesozoic deformation of the northern Transdanubian Range (Gerecse and Vértes Hills). *Acta Mineralogica-Petrographica, Field Guide Series*, 31: 1–52.

Fodor, L., Héja, G., Kövér, Sz., Csillag, G., and Csicsek, Á. L. (2017). Cretaceous deformation of the south-eastern Transdanubian Range Unit, and the effect of inherited Triassic–Jurassic normal faults. In: *Pre-conference Excursion Guide, 15th Meeting of the Central European Tectonic Studies Group (CETeG) 5–8th April 2017 Zánka, Lake Balaton*. Acta Mineralogica-Petrographica, Field Guide Series 32, pp. 47–76.

Fodor, L., Kercsmár, Zs., and Kövér, Sz. (2018). A Gerecse szerkezete és deformációs fázisai (Structure and deformation phases of the Gerecse). In: Budai T. (szerk.): *A Gerecse hegység földtana*. 169–208. In: Budai, T. (ed.): Geology of the Gerecse Mountains. – Mining and Geological Survey of Hungary, Budapest, 169–208, 370–386. ISBN 978-963-671-312-6.

Fodor, L., Balázs, A., Csillag, G., Dunkl, I., Héja, G., Jelen, B., Kelemen, P., Kövér, Sz., Németh, A., Nyíri, D., Selmeczi, I., Trajanova, M., Vrabec, M., and Vrabec, M. (2021). *Crustal exhumation and depocenter migration from the Alpine orogenic margin towards the Pannonian extensional back-arc basin controlled by inheritance*. Global and Planetary Change, p. 201, https://doi.org/10.1016/j.gloplacha.2021.103475.

Fruth, I. and Scherreiks, R. (1984). Hauptdolomit – Sedimentary and Paleogeographic models (Norian, Northern Calcareous Alps). *Geologische Rundschau*, 73(1): 305–319.

Fülöp, J. and Dank, V. (1987). *Magyarország földtani térképe, 1:500 000 – Magyar Állami Földtani Intézet*.

Galácz, A. (1988). Tectonically controlled sedimentation in the Jurassic of the Bakony Mountains (Transdanubian Central Range, Hungary). *Acta Geologica Hungarica*, 31: 313–328.

Galácz, A. and Vörös, A. (1972). A bakony-hegységi jura fejlődéstöneténeti vázlata a főbb üledékföldtani jelenségek kiértékelése alapján. (Jurassic history of the Bakony Mountains and interpretation of principal lithological phenomena, In Hungarian, with English abstract). *Földtani Közlöny*, 102: 122–135.

Góczán, F., Haas, J., Lőrincz, H., and Oravecz-Scheffer, A. (1983). *Keszthelyi-hegységi karni alapszelvény faciológiai és rétegtani értékelése (Hévíz-6. sz. fúrás). (Faciological and stratigraphic evaluation of a Carnian key section [borehole Hévíz-6], Keszthely Mountains, Hungary)*. Magyar Állami Földtani Intézet Évi Jelentése az 1981. Évről, pp. 263–293.

Haas, J. (1993). Formation and evolution of the „Kösseni Basin" in the Transdanubian Range. *Földtani Közlöny*, 123(1): 9–54.

Haas, J. (2002). Origin and evolution of Late Triassic backplatform and intraplatform basins in the Transdanubian Range, Hungary. *Geologica Carpathica*, 53(3): 159–178.

Haas, J., Jocháné-Edelényi, E., Gidai, L., Kaiser, M., Kretzoi, M., and Oravecz, J. (1984). Geology of the Sümeg Area. *Geologica Hungarica Series Geologica*, 20: 353.

Haas, J., Budai, T., and Raucsik, B. (2012). Climatic controls on sedimentary environments in the Triassic of the Transdanubian Range (Western Hungary). *Palaeogeography, Palaeoclimatology, Palaeoecology*, 353–355: 31–44, https://doi.org/10.1016/j.palaeo.2012.06.031.

Haas, J., Budai, T., Győri, O., and Kele, S. (2014). Multiphase partial and selective dolomitization of Carnian reef limestone (Transdanubian Range, Hungary). *Sedimentology*, 61(3): 836–859, http://doi.org/10.1111/sed.12088.

Haas, J., Budai, T., Hips, K., Czuppon, Gy., Győri, O., Horváth, A., and Héja, G. (2021). Dolomitization of Late Norian carbonate deposits of restricted basin facies in the Keszthely Mts., Transdanubian Range, Hungary. *International Journal of Earth Sciences*, 111: 245–268.

Héja, G. (2015). *A Keszthelyi-hegység és nyugati előterének szerkezetfejlődése, különös tekintettel a kréta deformációkra. (Structural evolution of the Keszthely hills and their western forelands, with aspect of the Cretaceous deformations, in Hungarian with English abstarct)*. MSc thesis, manuscript, Eötvös University, Dept. of Geology, p. 118.

Héja, G., Csizmeg, J., Kövér, Sz., and Fodor, L. (2016). *The effect of Late Triassic extension on eoalpine thrusting in the Keszthely Hills, West Hungary*. AAPG European Regional Conference and Exhibition, Bucharest, Romania, Abstract Volume, p. 154.

Héja, G., Csizmeg, J., Kövér, Sz., Németh, A., and Fodor, L. (2017). *Structural inheritance of Triassic–Jurassic normal faults in a Cretaceous thrust and fold belt based on seismic and field data (western Transdanubian Range, Hungary)*. 'Fold and Thrust Belts: structural style, evolution and exploration'. London, United Kingdom, Abstract Volume:, pp. 159–160.

Héja, G., Kövér, Sz., Csillag, G., Németh, A., and Fodor, L. (2018). Evidences for pre-orogenic passive-margin extension in a Cretaceous fold-and-thrust belt on the basis of combined seismic and field data (western Transdanubian Range, Hungary). *International Journal of Earth Sciences*, 107: 2955–2973, https://doi.org/10.1007/s00531-018-1637-3.

Héja, G., Ortner, H., Fodor, L., Németh, A., and Kövér, Sz. (2022). Modes of oblique inversion: a case study from the Cretaceous fold and thrust belt of the western Transdanubian Range (TR), West Hungary. *Tectonics*.

Hips, K., Haas, J., and Győri, O. (2015). Hydrothermal dolomitization of basinal deposits controlled by a synsedimentary fault system in Triassic extensional setting, Hungary. *International Journal of Earth Sciences (Geologishe Rundschau)*, 105: 1215–1231, https://doi.org/10.1007/s00531-015-1237-4.

Horváth, F., Musitz, B., Balázs, A., Végh, A., Uhrin, A., Nádor, A., Koroknai, B., Pap, N., Tóth, T., and Wórum, G. (2015). Evolution of the Pannonian basin and its geothermal resources. *Geothermics*, 53: 328–352.

Kelemen, P., Csillag, G., Dunkl, I., Mindszenty, A., Kovács, I., von Eynatten, H., and Józsa, S. (2021). Terrestrial kaolin deposits trapped in Miocene karstic sinkholes on planation surface remnants, Transdanubian Range, Pannonian Basin (Hungary). *Geological Magazine*, 158(2): 349–358.

Kiss, A (2009). *Az Északi-Bakony szerkezetalakulása*. PhD Thesis, Eötvös University, Dept. of Applied and Environmental Geology, p. 120.

Kiss, A. and Fodor, L. (2007). The Csesznek Zone in the northern Bakony Mts: a newly recognized transpressional element in dextral faults of the Transdanubian Range, western Hungary. *Geologica Carpathica*, 58(5): 465–475.

Kókay, J. (1956). Hegységszerkezeti viszonyok Várpalota környékén. *Földtani Közlöny*, 86(1): 17–29.

Kókay, J. (1996). A várpalotai neogén medence tektonikai összefoglalója. *Földtani Közlöny*, 126(4): 417–445.

Kókay, J. (1976). Geomechanical investigation of the southeastern margin of the Bakony Mountains and the Litér fault line. *Acta Geologica Hungarica*, 20: 245–257.

Lantos, Z. (1997). Karbonátos lejtő-üledékképződés egy liász tengeralatti magaslat oldalában, eltolódásos vetőzóna mentén (Gerecse). (Sediments of a Liassic carbonate slope controlled by strike-slip fault activity, Gerecse Hills, Hungary, in Hungarian with English abstract). *Földtani Közlöny*, 127(3–4): 291–320.

Márton, E. and Fodor, L. (2003). Tertiary paleomagnetic results and structural analysis from the Transdanubian Range (Hungary): sign for rotational disintegration of the Alcapa unit. *Tectonophysics*, 363: 201–224.

Mészáros, J. (1982). Nagyméretű vízszintes eltolódás a Bakony Ny-i részén és szerepe a nyersanyagkutatásban. *Földtani Intézet Évi Jelentése*, 1980: 517–526.

Mészáros, J. (1983). Structural and economic geological significance of strikeslip faults in the Bakony Mountains (in Hungarian with English abstract). *Földtani Intézet Évi Jelentése*, 1981: 485–502.

Miszlivecz, E., Turczi, G., and Koloszár, L. (1982). *Keszthely-Ny. Észlelési földtani térkép. A Balaton-felvidék földtani térképe 1:20 000-es sorozat*. Data Repository of the Mining and Geological Survey of Hungary.

Molnár, Zs., Kiss, G.B., Molnár, F., Váczi, T., Czuppon, Gy., Dunkl, I., Zaccarini, F., and Dódony, I. (2021). Epigenetic-Hydrothermal Fluorite Veins in a Phosphorite Deposit from Balaton Highland (Pannonian Basin, Hungary): Signatures of a Regional Fluid Flow System in an Alpine Triassic Platform. *Minerals*, 11: 1–21.

Nyíri, D., Tőkés, L., Zadravecz, Cs., and Fodor, L. (2021). Early post-rift confined turbidite systems in a supra-detachment basin: Implications for the early to middle Miocene basin evolution and hydrocarbon exploration of the Pannonian Basin. *Global and Planetary Change*, 203: 103500, https://doi.org/10.1016/j.gloplacha.2021.103500.

Ortner, H., Kositz, A., Willingshofer, E., and Sokoutis, D. (2015). Geometry of growth strata in a transpressive fold belt in field and analogue model: Gosau Group at Muttekopf, Northern Calcareous Alps, Austria. Basin Research, 2015: pp. 1–21.

Palotai, M., Csontos, L., and Dövényi, P. (2006). A kesztölci mezozoos (felső-jura) előfordulás terepi és geoelektromos vizsgálata (Field and geoelectric study of the Mesozoic (Upper Jurassic) occurrence at Kesztölc, in Hungarian with English abstract). *Földtani Közlöny*, 136(3): 347–368.

Petrik, A. (2016). *Structural evolution of the southern Bükk foreland (in Hungarian with English abstract)*. PhD thesis, Eötvös University Dept. of Geology, p. 208.

Petrik, A., Beke, B., Fodor, L., and Lukács, R. (2016). Cenozoic structural evolution of the southwestern Bükk Mts. and the southern part of the Darnó Deformation Belt (NE Hungary). *Geologica Carpathica*, 67(1): 83–104.

Pocsai, T. and Csontos, L. (2006). Late Aptian–early Albian syntectonic faciespattern of the Tata Limestone Formation (Transdanubian Range, Hungary). *Geologica Carpathica*, 57: 15–27.

Poros, Zs., Machel, H.G., Mindszenty, A., and Molnár, F. (2013). Cryogenic powderization of Triassic dolostones in the Buda Hills, Hungary. *International Journal of Earth Sciences*, 102: 1513–1539.

Royden, L., H. (1988). Late Cenozoic tectonics of the Pannonian basin system. In: Royden, L.H. and Horváth, F. (Eds.), *The Pannonian Basin, a Study in Basin Evolution*, Vol. 45. American Association of Petroleum Geologists, Memoir: pp. 27–48.

Rumpler, J. and Horváth, F. (1988). Some representative seismic reflection lines from the Pannonian basin and their structural interpretation. In: Royden, L.H. and Horváth, F. (Eds.), *The Pannonian Basin, a Study in Basin Evolution*, Vol. 45. American Association of Petroleum Geologists, Memoir, pp. 153–169.

Sasvári, Á. (2008). Rövidüléshez köthető deformációs jelenségek a Gerecse területén. (Shortening-related deformation in the Gerecse Mts, Transdanubian Range, Hungary, in Hungarian with English abstract). *Földtani Közlöny*, 138(4): 385–402.

Sasvári, Á. (2009). *Középső-kréta rövidüléses deformáció és szerkezeti betemetődés a Gerecse területén (in Hungarian, with English abstract)*. PhD thesis, Eötvös University, Dept. of Applied and General Geology, p. 164.

Sasvári, Á., Kiss, A., and Csontos, L. (2007). Paleostress investigation and kinematic analysis along the Telegdi Roth Fault (Bakony Mountains, western Hungary). *Geologica Carpathica*, 58: 477–486.

Sipos-Benkő, K., Márton, E., Fodor, L., and Pethe, M. (2014). An integrated magnetic susceptibility anisotropy (AMS) and structural geological study on Cenozoic clay rich sediments from the Transdanubian Range. *Central European Geology*, 51(1): 21–52, https://doi.org/10.1556/CEuGeol.57.2014.1.2.

Swierczewska, A., Tokarski, A., Banaś, M., and Fodor, L. (2007). *Why fractured clasts? – Meeting of the tectonic studies groups*. Glasgow, 05–06/01/2007, Geological Society, London.

Szentes, F. (1957). Bauxitkutatás a Keszthelyi-hegységben. *Földtani Intézet Évkönyve*, 46: 531–541.

Szives, O., Fodor, L., Fogarasi, A., and Kövér, S. (2018). Integrated calcareous nannofossil and ammonite data from the upper Barremian–lower Albian of the northeastern Transdanubian Range (central Hungary): Stratigraphical implications and consequences for dating tectonic events. *Cretaceous Research*, 91(4): 229–250.

Sztanó, O., Magyari, Á., and Tóth, P. (2010). Gilbert-type delta in the Pannonian Kálla Gravel near Tapolca, Hungary. *Földtani Közlöny*, 140(2): 167–182.

Tari, G. (1991). Multiple Miocene block rotation in the Bakony Mountains, Transdanubian Central Range, Hungary. *Tectonophysics*, 199: 93–108.

Tari, G. (1994). *Alpine tectonics of the Pannonian Basin*. PhD Thesis, Rice University, Houston, USA, p. 501.

Tari, G. and Horváth, F. (2010). Eo-Alpine evolution of the Transdanubian Range in the nappe system of the Eastern Alps: revival of a 15 years tectonic model. *Földtani Közlöny*, 140(4): 483–510.

Tari, G., Bada, G., Beidinger, A., Csizmeg, J., Danišik, M., Gjerazi, I., Grasemann, B., Kováč, M., Plašienka, D., Šujan, M., and Szafián, P. (2021). The connection between the Alps and the Carpathians beneath the Pannonian Basin: selective reactivation of Alpine nappe contacts during Miocene extension. *Global and Planetary Change*, 197, https://doi.org/10.1016/j.gloplacha.2020.103401.

Tari, G., Horváth, F., and Rumpler, J. (1992). Styles of extension in the Pannonian basin. *Tectonophysics*, 208: 203–219.

Teleki, G. (1939). Adatok Litér és környékének sztratigráfiájához és tektonikájához. *Földtani Intézet Évkönyve*, 32(1): 3–60.

Ustaszewski, K. and Schmid, S.M. (2006). Control of preexisting faults on geometry and kinematics in the northernmost part of the Jura fold-and-thrust belt. *Tectonics*, 25, https://doi.org/10.1029/2005TC001915.

Várkonyi, A., Törő, B., Sztanó, O., and Fodor, L. (2013). Late Cenozoic deformation and tectonically controlled sedimentation near the Balaton zone (central Pannonian basin, Hungary). *Occasional Papers of the Geological and Geophysical Institute of Hungary*, 1: 72–73. ISSN 2064-0293, ISBN 978-963-671-294-5.

Visnovitz, F., Horváth, F., Fekete, N., and Spiess, V. (2015). Strike-slip tectonics in the Pannonian basin based on seismic surveys at Lake Balaton. *International Journal of Earth Sciences*, 104: 2273–2285, https://doi.org/10.1007/s00531-015-1179-x.

Vörös, A. and Galácz, A. (1998). Jurassic palaeogeography of the Transdanubian Central Range (Hungary). *Rivista Italiana di Paleontologia e Stratigrafia*, 104(1): 69–84.

Winterer, E.L., Metzler, C.V., and Sarti, M. (1991). Neptunian dykes and associated breccias (Southern Alps, Italy and Switzerland): role of gravity sliding in open and closed systems. *Sedimentology*, 38: 381–404.

Zámolyi, A., Kovács, G., Székely, B., and Tímár, G. (2010). A morphometric analysis of the fault pattern of the Bakony Mountains: some tectonic geomorphological implications (in Hungarian, with English abstract). *Földtani Közlöny*, 140(4): 439–453.